

## **Ferrocene-BODIPY-merocyanine triads: new NIR absorbing platforms with optical properties susceptible to protonation**

**Yuriy V. Zatsikha,<sup>a</sup> Natalia O. Didukh,<sup>b</sup> Dion Nemez,<sup>a</sup> Adrien C. Schlachter,<sup>c</sup> Paul-Ludovic Karsenti,<sup>c</sup> Yuriy P. Kovtun,<sup>\*b</sup> Pierre D. Harvey,<sup>\*c</sup> and Victor N. Nemykin<sup>\*a,d</sup>**

### **SUPPORTING INFORMATION**

# CONTENTS

GENERAL EXPERIMENTAL	4
EXPERIMENTAL PROCEDURE	6
Figure S1. $^1\text{H}$ NMR spectrum of compound <b>2</b> in $\text{CDCl}_3$	8
Figure S2. COSY NMR spectrum of compound <b>2</b> in $\text{CDCl}_3$	8
Figure S3. $^{13}\text{C}$ NMR spectrum of compound <b>2</b> in $\text{CDCl}_3$	9
Figure S4. $^1\text{H}$ NMR spectrum of compound <b>3</b> in $\text{CDCl}_3$	9
Figure S5. COSY NMR spectrum of compound <b>3</b> in $\text{CDCl}_3$	10
Figure S6. $^{13}\text{C}$ NMR spectrum of compound <b>3</b> in $\text{CDCl}_3$	10
Figure S7. $^1\text{H}$ NMR spectrum of compound <b>4</b> in $\text{CDCl}_3$	11
Figure S8. COSY NMR spectrum of compound <b>4</b> in $\text{CDCl}_3$	11
Figure S9. $^{13}\text{C}$ NMR spectrum of compound <b>4</b> in $\text{CDCl}_3$	12
Figure S10. $^1\text{H}$ NMR spectrum of compound <b>5</b> in $\text{CDCl}_3$	12
Figure S11. COSY NMR spectrum of compound <b>5</b> in $\text{CDCl}_3$	13
Figure S12. $^{13}\text{C}$ NMR spectrum of compound <b>5</b> in $\text{CDCl}_3$	13
Figure S13. $^1\text{H}$ NMR spectrum of compound <b>6</b> in $\text{CDCl}_3$	14
Figure S14. COSY NMR spectrum of compound <b>6</b> in $\text{CDCl}_3$	14
Figure S15. $^{13}\text{C}$ NMR spectrum of compound <b>6</b> in $\text{CDCl}_3$	15
Figure S16. The comparison of the normalized UV-vis spectra of protonated dyes $[\mathbf{5}+\text{H}]^+$ and $[\mathbf{6}+\text{H}]^+$ with Fc-BODIPY dyad.	16
Figure S17. UV-Vis-NIR and TDDFT-predicted UV-vis spectra of protonated dyes $[\mathbf{5}+\text{H}]^+$ and $[\mathbf{6}+\text{H}]^+$ .	17
Figure S18. Transformation of $[\mathbf{5}+\text{H}]^+$ and $[\mathbf{6}+\text{H}]^+$ into corresponding <b>5</b> and <b>6</b> under TEA titrations in DCM.	18
Figure S19. DFT SP predicted MOs composition for triads <b>5</b> and <b>6</b> .	19
Figure S20. Decay associated spectra of <b>5</b> ( $\lambda_p=800\text{nm}$ , $\lambda_{pr}=460\text{nm}$ ).	20
Figure S21. Decay associated spectra of <b>5</b> ( $\lambda_p=800\text{nm}$ , $\lambda_{pr}=460\text{nm}$ ).	21
Figure S22. Transient absorption map of <b>5</b> ( $\lambda_p=800\text{nm}$ , $\lambda_{pr}=460\text{nm}$ ) over a 7ns window.	22

<b>Figure S23.</b> Transient absorption map of <b>5</b> ( $\lambda_p=800\text{nm}$ , $\lambda_{pr}=460\text{nm}$ ) over an 8ps window.	<b>23</b>
<b>Figure S24.</b> Transient absorption kinetics of <b>5</b> ( $\lambda_p=800\text{nm}$ , $\lambda_{pr}=460\text{nm}$ ) at different wavelengths on an 8ps window.	<b>24</b>
<b>Figure S25.</b> Decay associated spectra of <b>6</b> ( $\lambda_p=800\text{nm}$ , $\lambda_{pr}=460\text{nm}$ ).	<b>24</b>
<b>Figure S26.</b> Transient absorption map of <b>6</b> ( $\lambda_p=800\text{nm}$ , $\lambda_{pr}=460\text{nm}$ ) over a 7ns window.	<b>25</b>
<b>Figure S27.</b> Transient absorption spectra of <b>6</b> ( $\lambda_p=800\text{nm}$ , $\lambda_{pr}=460\text{nm}$ ) at different times.	<b>25</b>
<b>Figure S28.</b> Transient absorption kinetics of <b>6</b> ( $\lambda_p=800\text{nm}$ , $\lambda_{pr}=460\text{nm}$ ) at different wavelengths on an 8ps window.	<b>26</b>
<b>Figure S29.</b> DFT-PCM predicted spin density distribution of cation <b>6</b> <sup>+</sup> .	<b>26</b>
<b>Table S1.</b> DFT optimized geometries and energies of protonated dyes [ <b>5</b> +H] <sup>+</sup> and [ <b>6</b> +H] <sup>+</sup>	<b>27</b>
<b>Table S2.</b> Redox properties of triads <b>5</b> and <b>6</b> in DCM.	<b>29</b>
<b>REFERENCES</b>	<b>30</b>

## GENERAL INFORMATION.

**Reagents and materials.** Solvents were purified using standard approaches: toluene was dried over sodium metal, DCM was dried over calcium hydride, DMF was dried over P<sub>2</sub>O<sub>5</sub>. Ferrocene carboxaldehyde was purchased from Sigma Aldrich, BODIPY derivative **1** <sup>[1]</sup> and quaternary heterocycle ammonium salts <sup>[2]</sup> were prepared as described earlier.

**Spectroscopy Measurements.** Jasco-720 spectrophotometer was used to collect UV-Vis data. Electrochemical cyclic voltammetry (CV) and differential pulse voltammetry (DPV) measurements were conducted using a CH Instruments electrochemical analyzer utilizing a three-electrode scheme with platinum working, auxiliary and Ag/AgCl reference electrodes. DCM was used as solvents and 0.1 M solution of tetrabutylammonium perchlorate (TBAP) was used as supporting electrolyte. In all cases, experimental redox potentials were corrected using decamethylferrocene (Fc\*H) as an internal standard. NMR spectra were recorded on a Bruker Avance instrument with a 300 MHz frequency for protons and 75 MHz frequency for carbons. Chemical shifts are reported in parts per million (ppm) and referenced to tetramethylsilane (Si(CH<sub>3</sub>)<sub>4</sub>) as an internal standard. High-resolution mass spectra of compounds **5** and **6** were recorded using a Bruker micrOTOF-QIII.

**Photophysics.** All the data analyses are done using the free software Glotaran that allows global analysis of the transient absorption maps. For a fixed amount of expected lifetimes, the global analysis iterates to find the best set of  $\tau_i$  fitting for all wavelengths and their respective coefficients  $C_i$ . The fit can be seen as a simple sum of exponentials:

$$I(\lambda, t) = C_1(\lambda) \cdot e^{(-t/\tau_1)} + C_2(\lambda) \cdot e^{(-t/\tau_2)} + \dots$$

In this equation, the coefficients  $C_i$  represent the "Decay associated spectra" for  $\tau_i$  (DAS). The instrument response function (IRF) and the white light continuum temporal chirp are also deconvolved to give the best regression fitting the whole 3D transient absorption map. In contrast to TCSPC measurements, the standard deviation over transient absorption data is not predefined and depends on a considerable amounts of factors. To evaluate the goodness of the fit, the root mean squared error (RMSE) is shown in the legend of the DAS spectra.

**Computational Details.** The starting geometry of compounds **5**, **6**, [**5**+H]<sup>+</sup> and [**6**+H]<sup>+</sup> were optimized using a B3LYP exchange-correlation functional.<sup>[3]</sup> This B3LYP exchange-correlation functional was found to result in good agreement between calculated and experimentally determined bond distances and angles in ferrocene-containing compounds.<sup>[4]</sup> Energy minima in optimized geometry was confirmed by the frequency calculations (absence of the imaginary frequencies). Solvent effect was

calculated using the polarized continuum model (PCM).<sup>[5]</sup> In all calculations, DCM was used as the solvent. In PCM-TDDFT calculation, the first 50 states were calculated. Full-electron Wachter's basis set <sup>[6]</sup> was utilized for iron atoms, while all other atoms were modeled using 6-31G(d) <sup>[7]</sup> basis set. Gaussian 09 software was used in all calculations.<sup>[8]</sup> QMForge program was used for molecular orbital analysis.<sup>[9]</sup>

## EXPERIMENTAL PROCEDURE.

**Compound 2.** The mixture of compound **1** (570 mg, 0.866 mmol), ferrocene carboxaldehyde (315 mg, 1.47 mmol), acetic acid (519 mg, 8.66 mmol) and piperidine (220 mg, 2.6 mmol) in toluene (10 mL) was refluxed for 3 h. Then the solution was washed with water, organic layer was dried over Na<sub>2</sub>SO<sub>4</sub> and evaporated to dryness. The crude product was washed with methanol and purified by flash column chromatography on silica gel using DCM as a solvent yielding 500 mg (67.5 %) of compound **2**. <sup>1</sup>H NMR (300 MHz, CDCl<sub>3</sub>) δ 7.74 (d, *J*<sub>H,H</sub> = 16.0 Hz, 1H), 7.42-7.29 (m, 11H), 6.94 (s, 1H), 4.93 (t, *J*<sub>H,H</sub> = 5.7 Hz, 1H), 4.66 (t, *J*<sub>H,H</sub> = 1.8 Hz, 2H), 4.52 (t, *J*<sub>H,H</sub> = 1.8 Hz, 2H), 4.26 (s, 5H), 4.21-4.12 (m, 4H), 3.78-3.70 (m, 4H), 3.57-3.47 (m, 2H); 1.19-1.13 (m, 6H), 1.05 (t, *J*<sub>H,H</sub> = 7.1 Hz, 3H); <sup>13</sup>C NMR (75 MHz, CDCl<sub>3</sub>) δ 165.11, 164.38, 156.11, 147.15, 144.18, 135.34, 133.48, 132.31, 131.88, 130.14, 129.67, 129.05, 128.67, 128.39, 128.13, 126.47, 123.02, 122.75, 114.45, 102.73, 81.83, 71.60, 70.43, 70.19, 68.87, 62.81, 61.17, 60.47, 33.34, 29.86, 15.38, 14.05, 13.89.

**Compound 3.** The mixture of compound **2** (470 mg, 0.55 mmol) and concentrated hydrochloric acid (1 mL) in THF (10 mL) was refluxed for 5 min. After cooling to room temperature, the solution was diluted with water (20 mL) and stirred for 30 min. The resulting precipitate was filtered, washed with water and dried. Yield 375 mg (92 %). <sup>1</sup>H NMR (300 MHz, CDCl<sub>3</sub>) δ 9.83 (s, 1H), 7.79 (d, *J*<sub>H,H</sub> = 16.0 Hz, 1H), 7.42-7.29 (m, 11H), 6.95 (s, 1H), 4.68 (t, *J*<sub>H,H</sub> = 1.8 Hz, 2H), 4.58 (t, *J*<sub>H,H</sub> = 1.8 Hz, 2H), 4.50 (s, 2H), 4.27 (s, 5H), 4.21-4.09 (m, 4H), 1.11-1.04 (m, 6H); <sup>13</sup>C NMR (75 MHz, CDCl<sub>3</sub>) δ 196.17, 164.91, 163.69, 156.02, 150.39, 148.47, 146.40, 143.67, 136.68, 133.44, 132.43, 131.38, 130.41, 129.60, 129.39, 128.66, 128.51, 127.90, 126.25, 123.96, 119.94, 114.05, 81.49, 72.24, 70.43, 69.20, 61.41, 60.47, 43.49, 30.52, 13.96, 13.87.

**Compound 4.** The mixture of compound **3** (260 mg, 0.351 mmol) and DMF (26 mg, 0.351 mmol) in acetic anhydride (5 mL) was refluxed for 5 min. After cooling to room temperature, the solid was filtered and washed with ethanol. Yield 198 mg (72 %). <sup>1</sup>H NMR (300 MHz, CDCl<sub>3</sub>) δ 8.74 (d, *J*<sub>H,H</sub> = 12.8 Hz, 1H), 7.76 (d, *J*<sub>H,H</sub> = 16.0 Hz, 1H), 7.42-7.29 (m, 11H), 7.18 (d, *J*<sub>H,H</sub> = 12.8 Hz, 1H), 6.88 (s, 1H), 4.69 (t, *J*<sub>H,H</sub> = 1.8 Hz, 2H), 4.54 (t, *J*<sub>H,H</sub> = 1.8 Hz, 2H), 4.27 (s, 5H), 4.21-4.09 (m, 4H), 2.27 (s, 3H), 1.09-0.99 (m, 6H); <sup>13</sup>C NMR (75 MHz, CDCl<sub>3</sub>) δ 167.31, 165.15, 164.71, 145.83, 144.88, 135.97, 134.40, 132.52, 131.83, 129.82, 129.65, 129.11, 128.68, 128.43, 128.22, 124.80, 114.41, 105.54, 81.84, 71.82, 70.31, 68.99, 61.26, 61.00, 20.98, 13.90, 13.78.

### Compounds 5 and 6.

The mixture of compound **4** (100 mg, 0.127 mmol), *N*-methyl heterocyclic quaternary ammonium salt (0.127 mmol), and DIPEA (33 mg, 0.255 mmol) was refluxed in *i*-PrOH (5 mL) for 10 min. After cooling to room temperature, the solution was diluted with water (10) and stirred for another 30 min. The precipitate was filtered, washed

with water and methanol. The crude was purified by flash column chromatography on silica gel using DCM as a solvent.

**Compound 5:** (85 mg, yield 75%);  $^1\text{H}$  NMR (300 MHz,  $\text{CDCl}_3$ )  $\delta$  8.59 (dd,  $J_{\text{H,H}} = 14.7, 12.4$  Hz, 1H), 7.49-7.48 (m, 2H), 7.38-7.28 (m, 11H), 7.23-7.22 (m, 2H), 7.12 (d,  $J_{\text{H,H}} = 14.7$  Hz, 1H), 7.012 (t,  $J_{\text{H,H}} = 7.8$  Hz, 1H), 6.82 (d,  $J_{\text{H,H}} = 7.8$  Hz, 1H), 6.65 (s, 1H), 5.85 (d,  $J_{\text{H,H}} = 12.4$  Hz, 1H), 4.64 (t,  $J_{\text{H,H}} = 1.8$  Hz, 2H), 4.43 (t,  $J_{\text{H,H}} = 1.8$  Hz, 2H), 4.24 (s, 5H), 4.20-4.07 (m, 4H), 3.32 (s, 3H), 1.75 (s, 6H), 1.06 (t,  $J_{\text{H,H}} = 7.2$  Hz, 3H), 0.95 (t,  $J_{\text{H,H}} = 7.2$  Hz, 3H);  $^{13}\text{C}$  NMR (75 MHz,  $\text{CDCl}_3$ )  $\delta$  166.07, 165.64, 165.13, 144.33, 140.35, 138.59, 133.57, 133.21, 132.64, 129.82, 129.56, 128.63, 128.19, 128.12, 128.08, 121.94, 121.70, 119.59, 115.89, 112.06, 107.58, 100.79, 83.02, 70.44, 69.94, 68.14, 60.86, 60.79, 47.24, 29.79, 28.48, 13.95, 13.79;  $\lambda_{\text{max}}$  ( $\text{CH}_2\text{Cl}_2$ )/nm 370, 439, 493 and 809 ( $\epsilon/\text{dm}^3 \text{ mol}^{-1} \text{ cm}^{-1}$  32 000, 37 500, 19 300 and 65 000); HRMS (ESI positive) calcd for  $\text{C}_{53}\text{H}_{48}\text{BF}_2\text{FeN}_3\text{O}_4$  [ $\text{M} + \text{H}$ ] $^+$ : 895.3060, found 895.2903.

**Compound 6:** (65 mg, yield 65%);  $^1\text{H}$  NMR (300 MHz,  $\text{CDCl}_3$ )  $\delta$  8.20 (dd,  $J_{\text{H,H}} = 14.6, 11.8$  Hz, 1H), 7.63-7.28 (m, 14 H), 7.13-6.99 (m, 3H), 6.60 (s, 1H), 5.96 (d,  $J_{\text{H,H}} = 11.8$  Hz, 1H), 4.67 (t,  $J_{\text{H,H}} = 1.8$  Hz, 2H), 4.41 (t,  $J_{\text{H,H}} = 1.8$  Hz, 2H), 4.24 (s, 5H), 4.20-4.11 (m, 4H), 3.50 (s, 3H), 1.07-1.00 (m, 6H);  $^{13}\text{C}$  NMR (75 MHz,  $\text{CDCl}_3$ )  $\delta$  165.93, 165.77, 156.60, 142.77, 138.40, 137.24, 133.49, 132.45, 129.88, 129.57, 128.67, 128.23, 128.09, 127.96, 127.02, 122.81, 121.88, 118.75, 115.87, 110.36, 109.94, 97.10, 83.28, 70.32, 69.95, 68.16, 61.10, 60.62, 32.04, 13.95, 13.86;  $\lambda_{\text{max}}$  ( $\text{CH}_2\text{Cl}_2$ )/nm 368, 445, 490 and 814 ( $\epsilon/\text{dm}^3 \text{ mol}^{-1} \text{ cm}^{-1}$  24 400, 34 000, 16 000 and 56 000); HRMS (ESI positive) calcd for  $\text{C}_{50}\text{H}_{42}\text{BF}_2\text{FeN}_3\text{O}_4\text{S}$  [ $\text{M} + \text{H}$ ] $^+$ : 885.2310, found 885.2180.

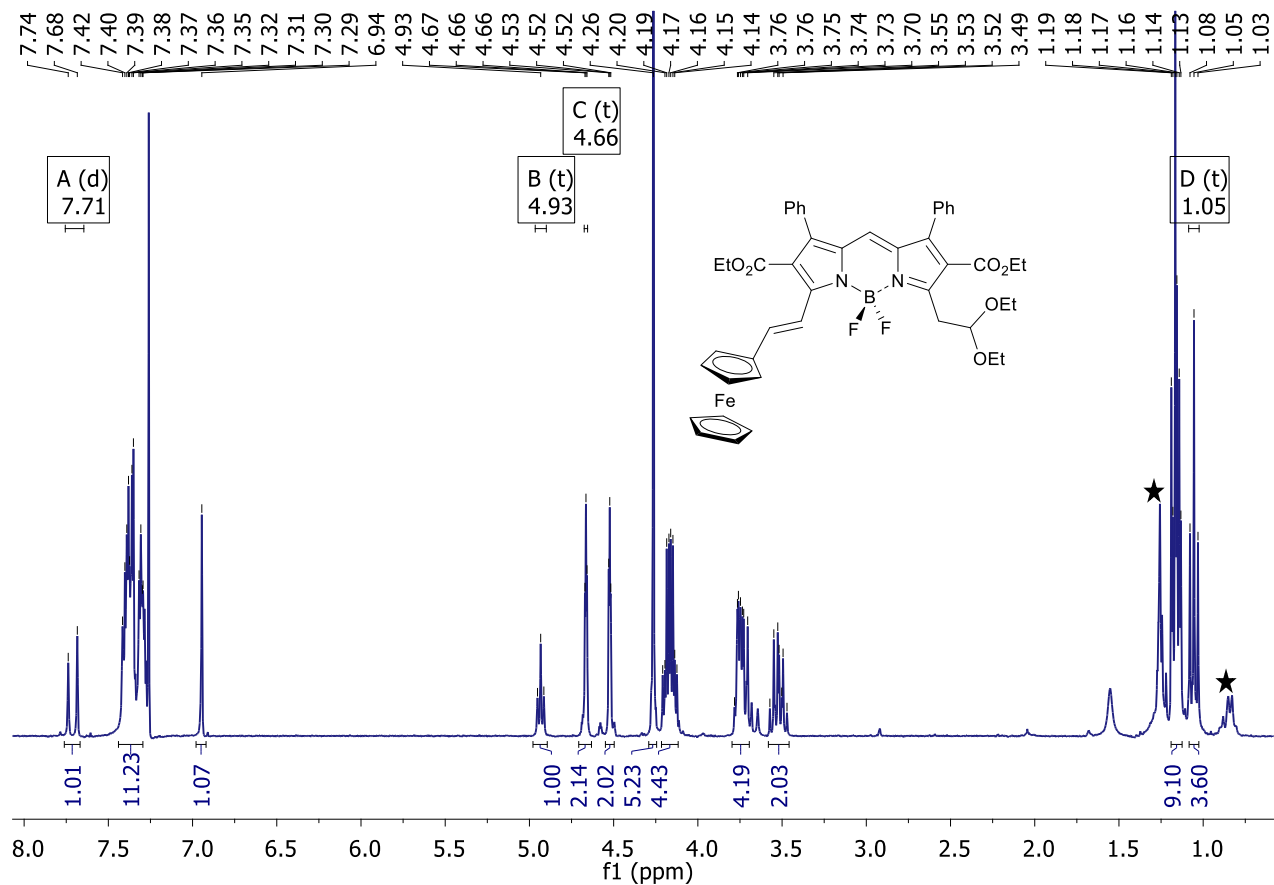


**Figure S1.**  $^1\text{H}$  NMR spectrum of compound **2** in  $\text{CDCl}_3$ . (★denote solvent residues).

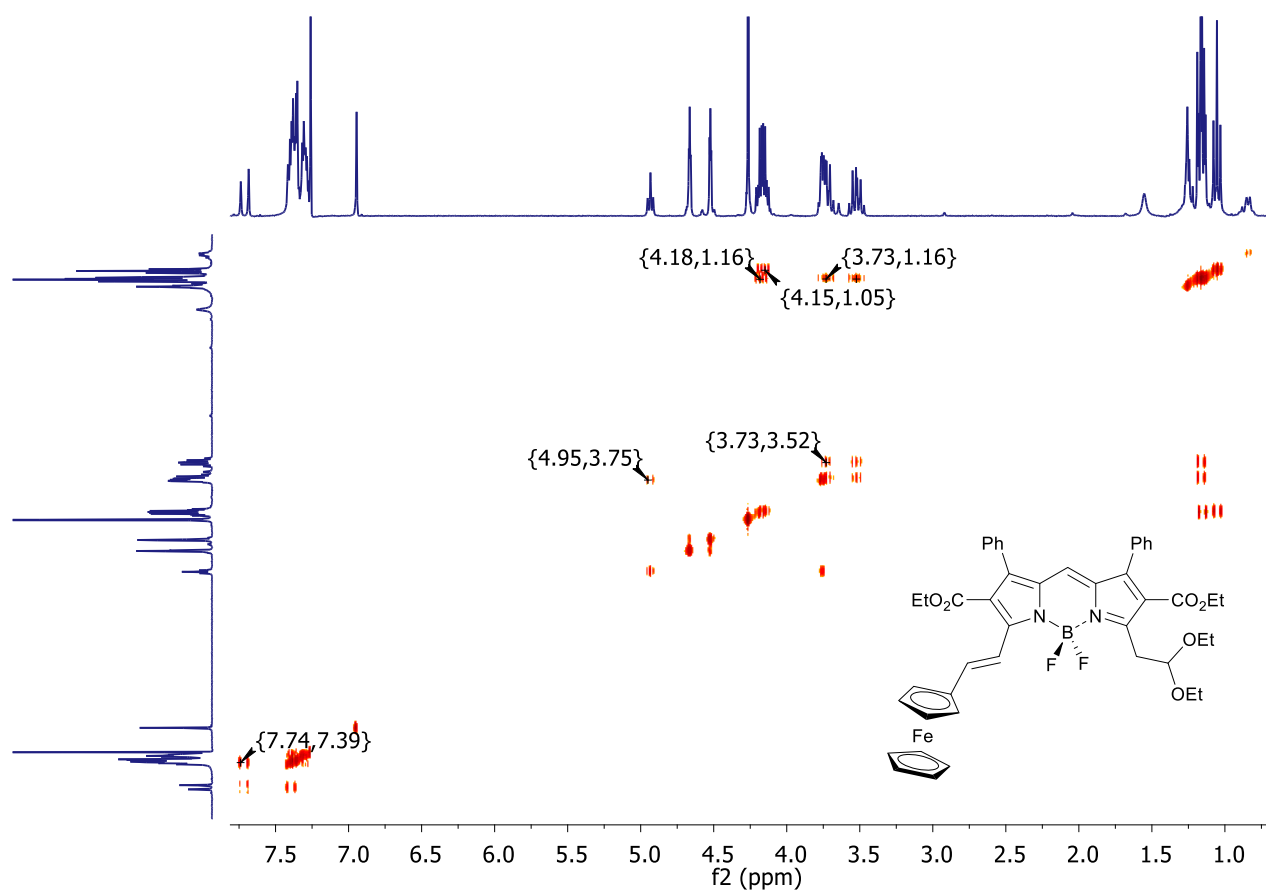


**Figure S2.** COSY NMR spectrum of compound **2** in  $\text{CDCl}_3$ .



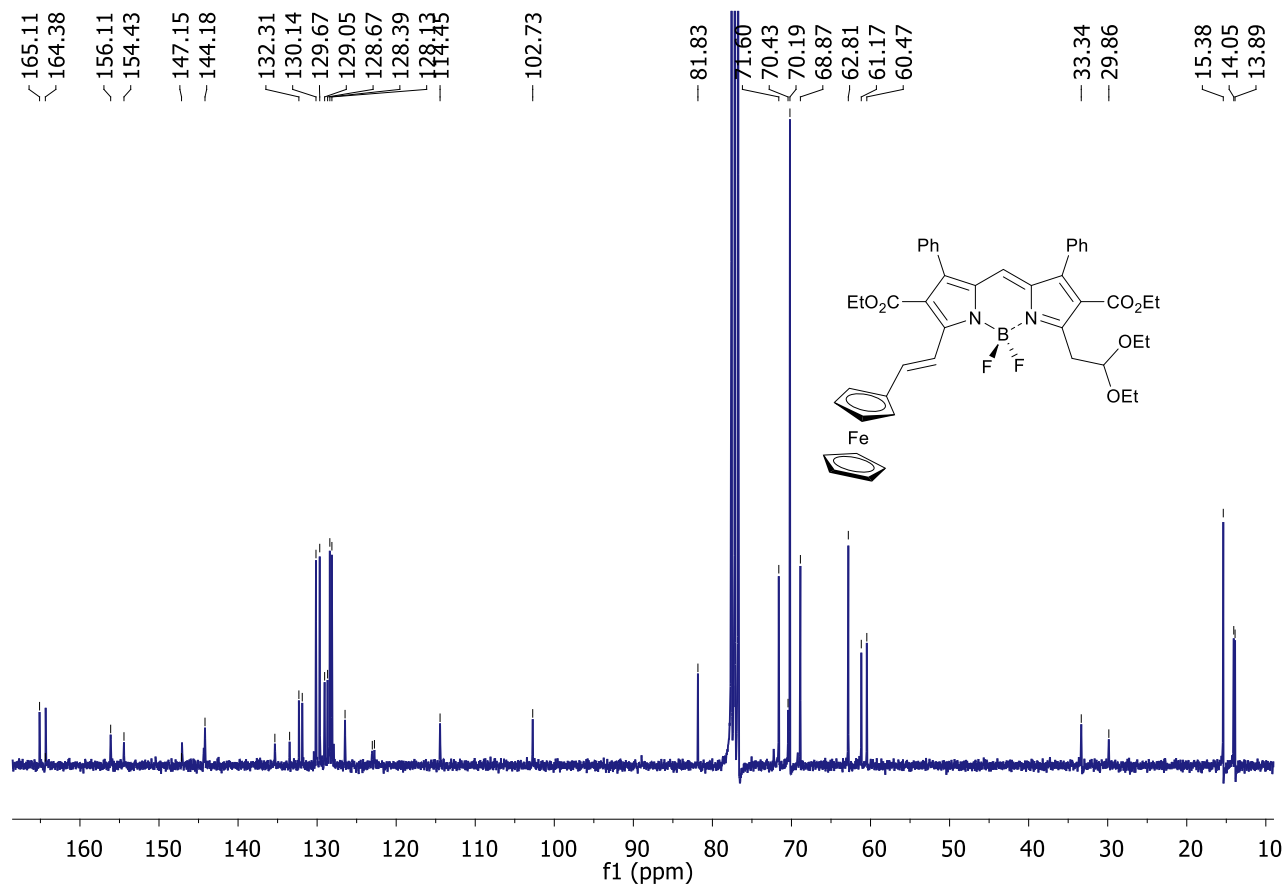


**Figure S3.**  $^{13}\text{C}$  NMR spectrum of compound **2** in  $\text{CDCl}_3$ .

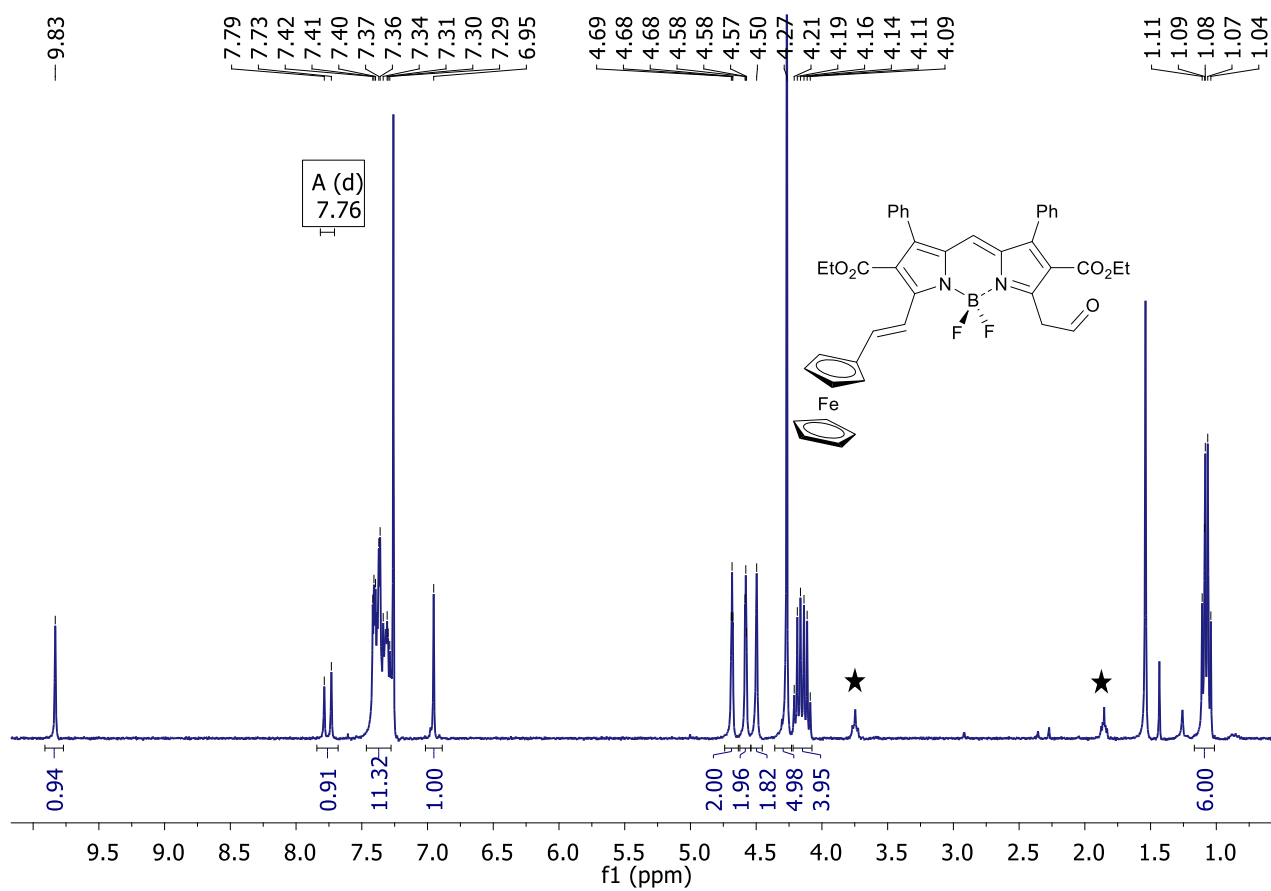


**Figure S4.**  $^1\text{H}$  NMR spectrum of compound **3** in  $\text{CDCl}_3$ . (★denote solvent residues).

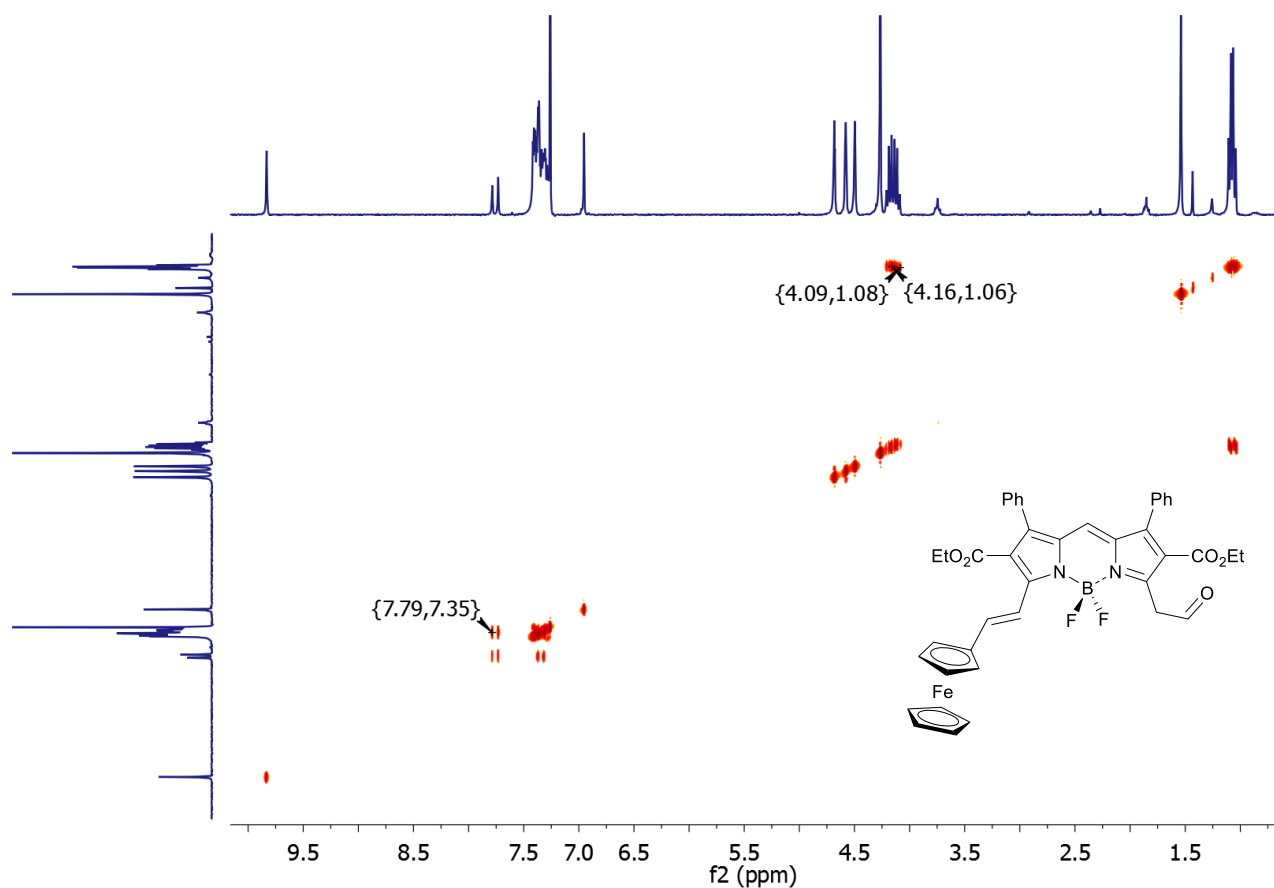


**Figure S5.** COSY NMR spectrum of compound **3** in  $\text{CDCl}_3$ .

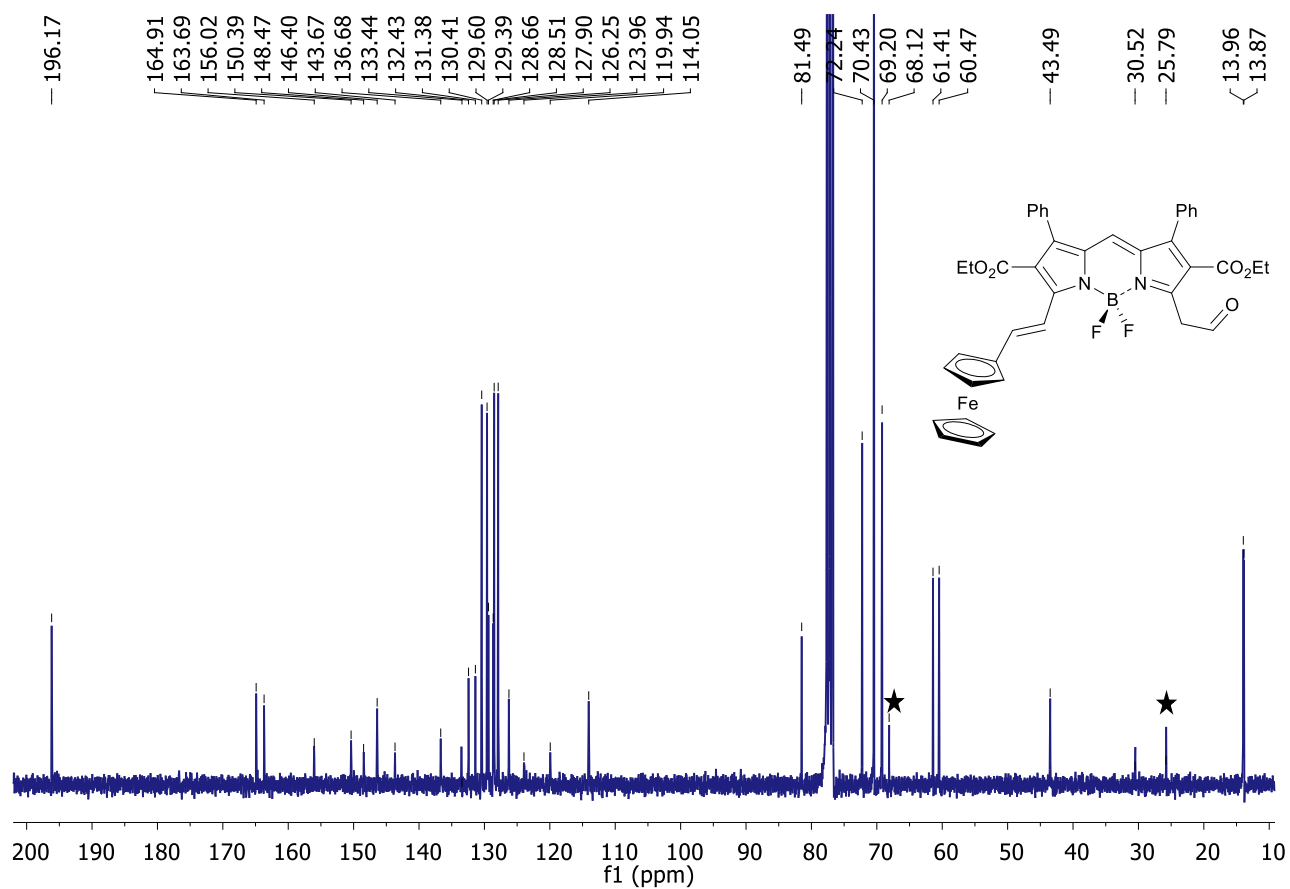


**Figure S6.**  $^{13}\text{C}$  NMR spectrum of compound **3** in  $\text{CDCl}_3$ . (★ denote solvent residues).

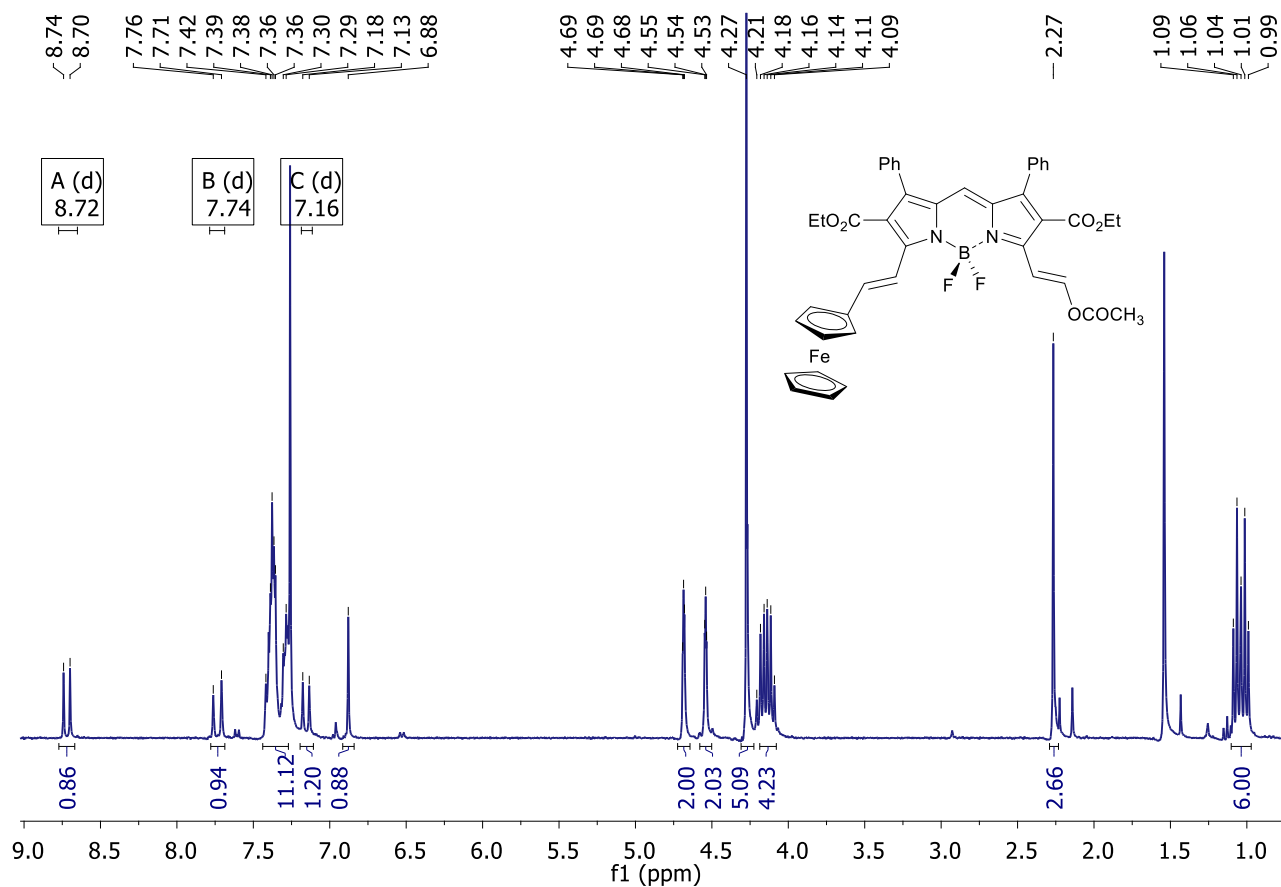


**Figure S7.**  $^1\text{H}$  NMR spectrum of compound **4** in  $\text{CDCl}_3$ .

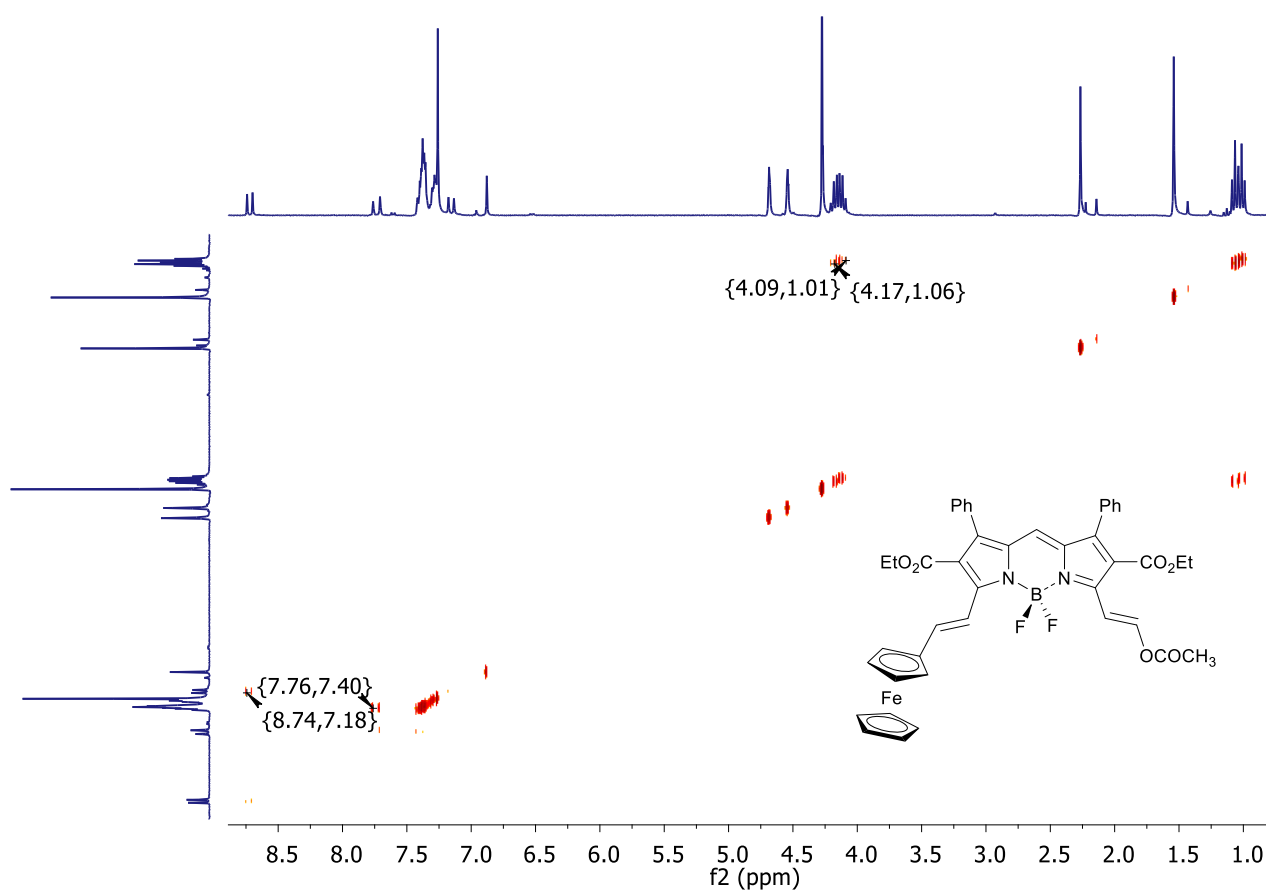


**Figure S8.** COSY NMR spectrum of compound **4** in  $\text{CDCl}_3$ .

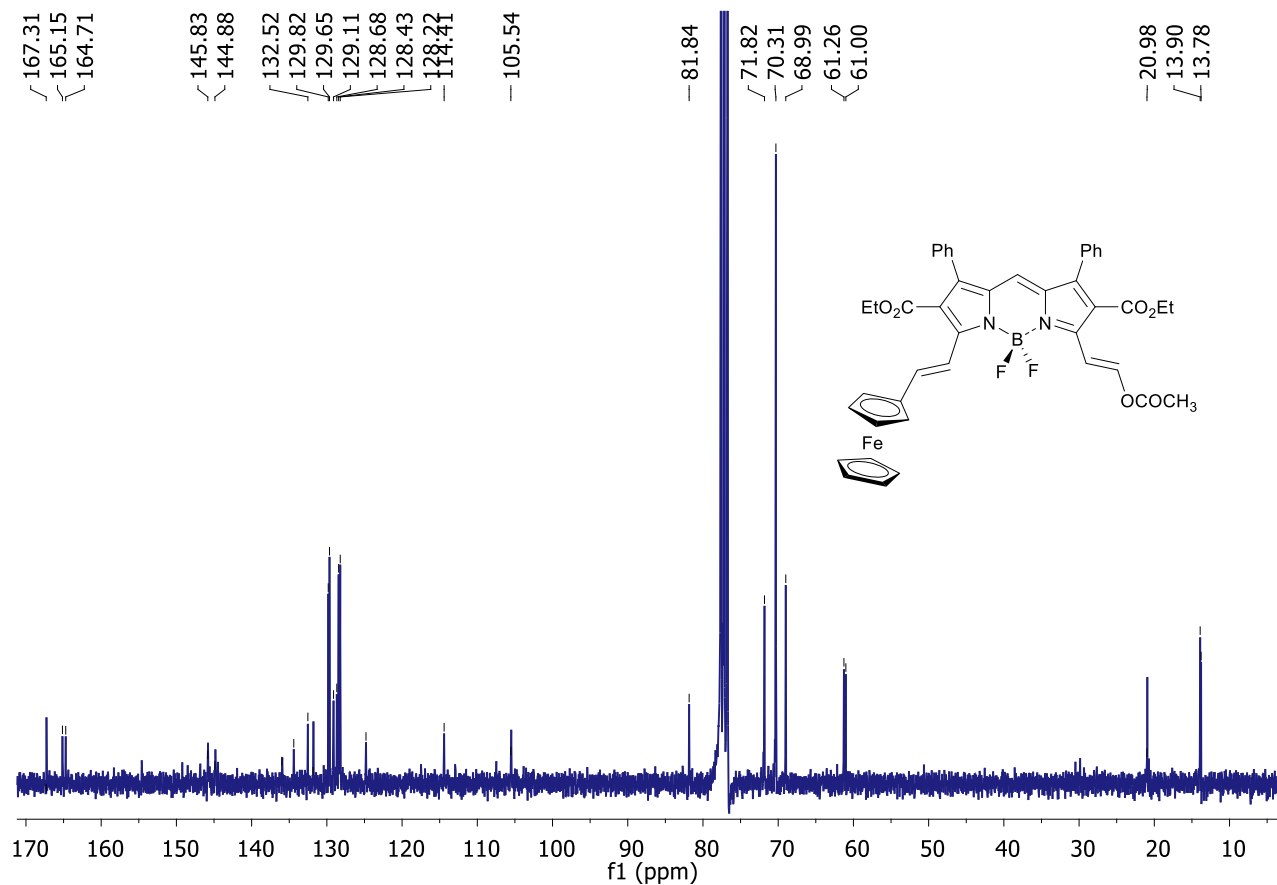


**Figure S9.** <sup>13</sup>C NMR spectrum of compound **3** in CDCl<sub>3</sub>.

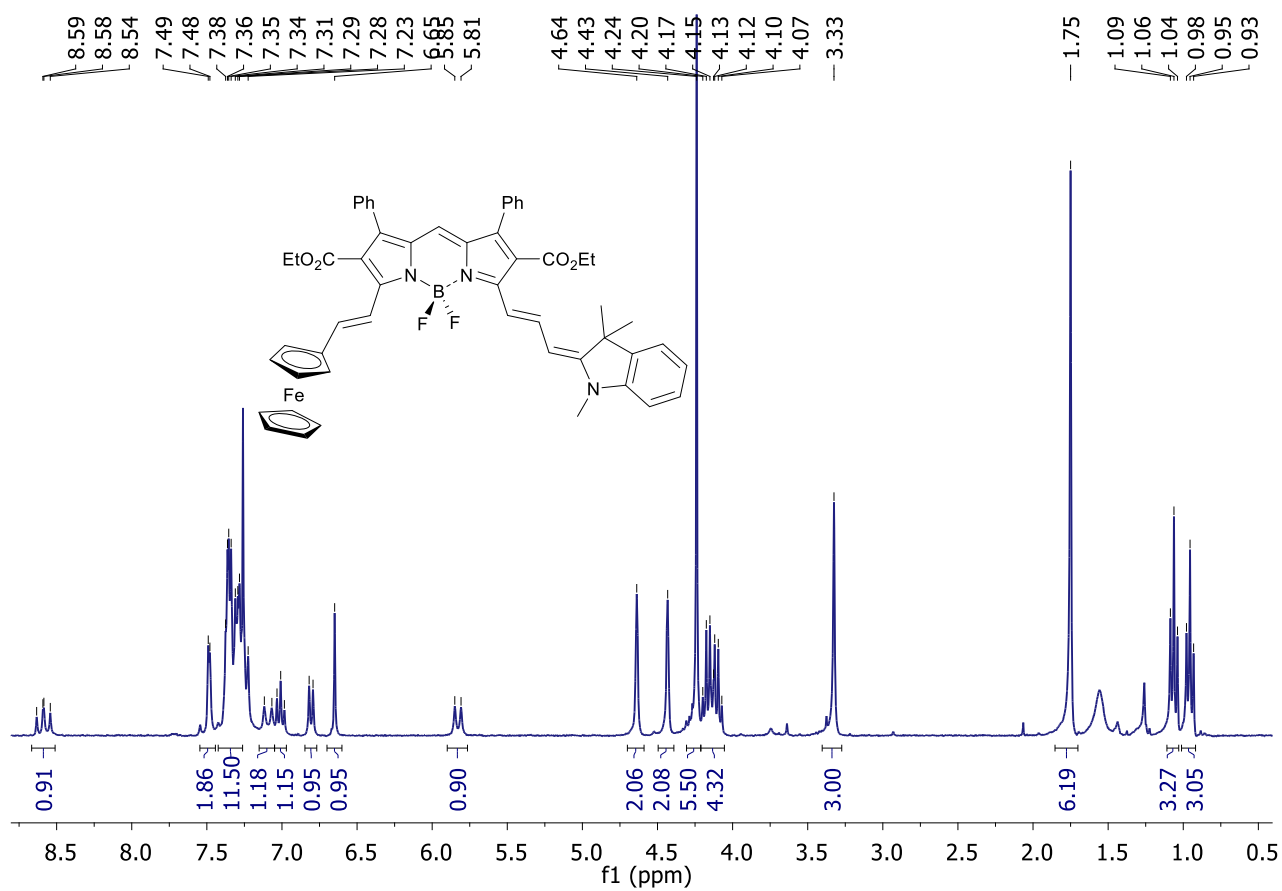


**Figure S10.** <sup>1</sup>H NMR spectrum of compound **5** in CDCl<sub>3</sub>.

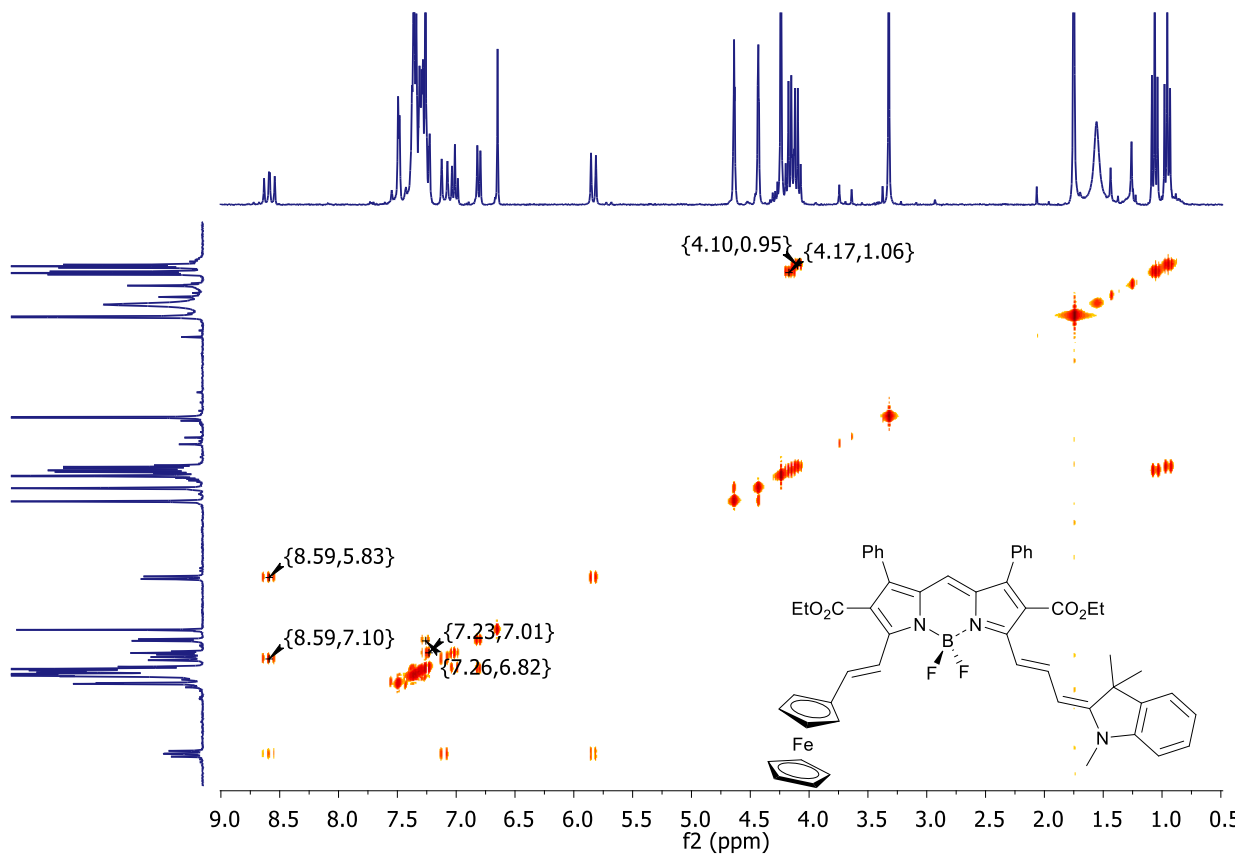


**Figure S11.** COSY NMR spectrum of compound **5** in  $\text{CDCl}_3$ .

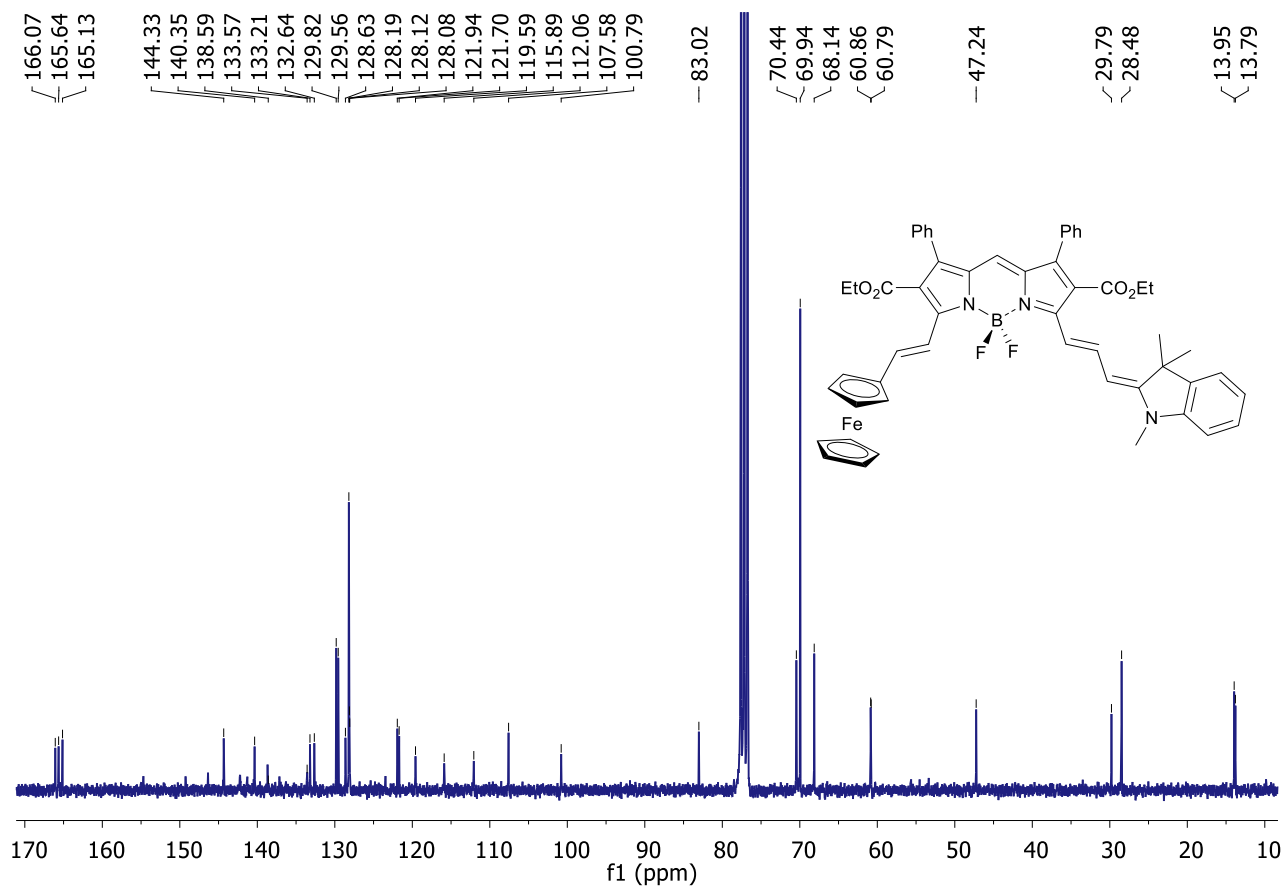


**Figure S12.**  $^{13}\text{C}$  NMR spectrum of compound **5** in  $\text{CDCl}_3$ .

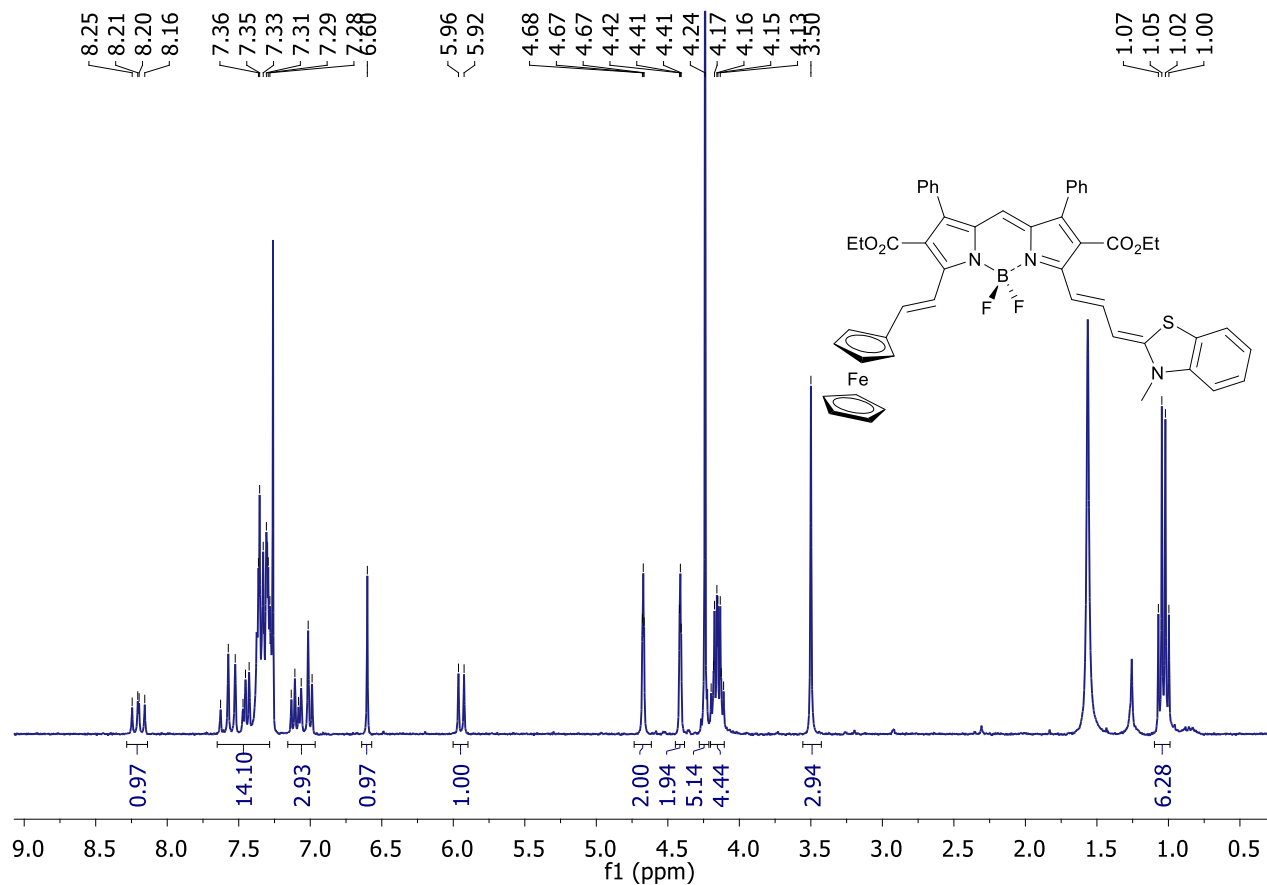


**Figure S13.**  $^1\text{H}$  NMR spectrum of compound **6** in  $\text{CDCl}_3$ .

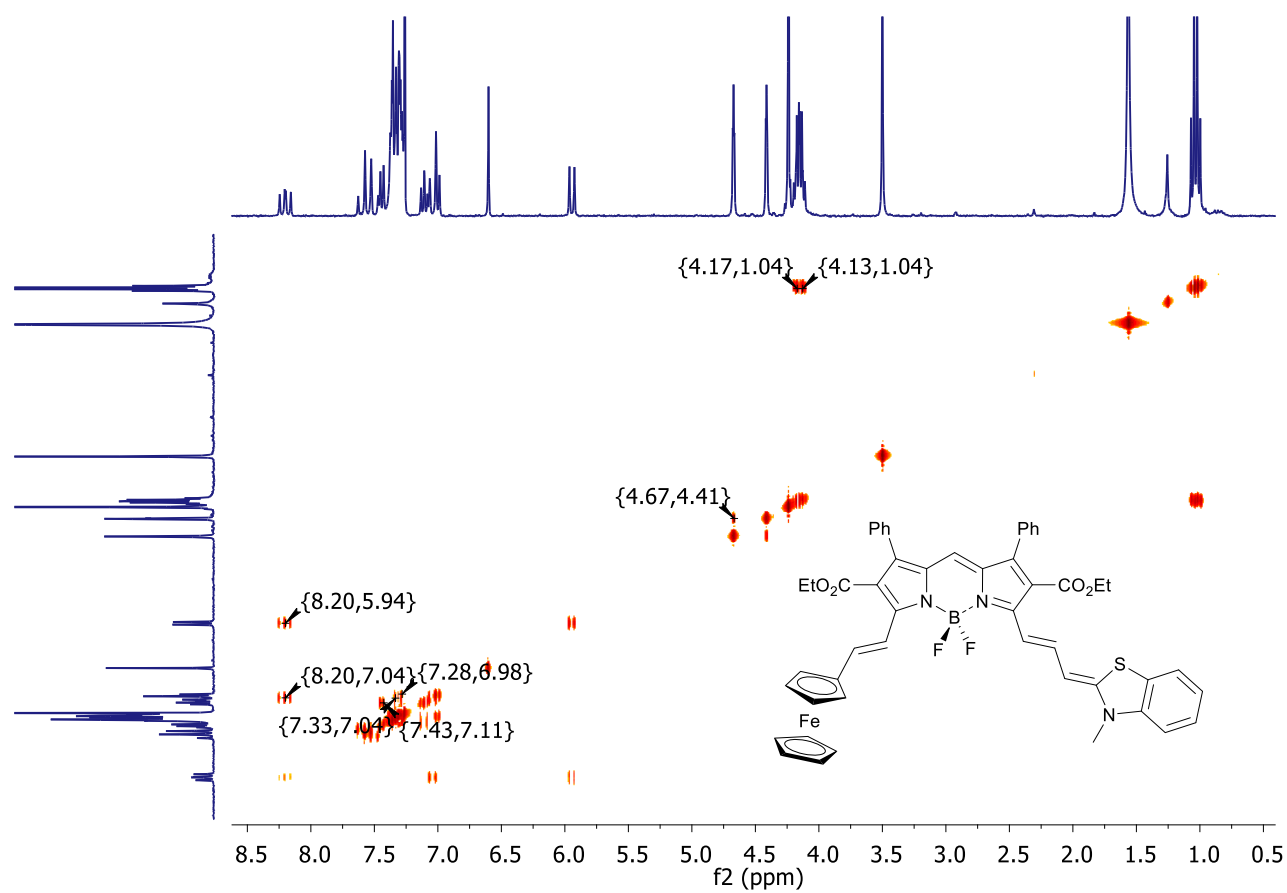


**Figure S14.** COSY NMR spectrum of compound **6** in  $\text{CDCl}_3$ .

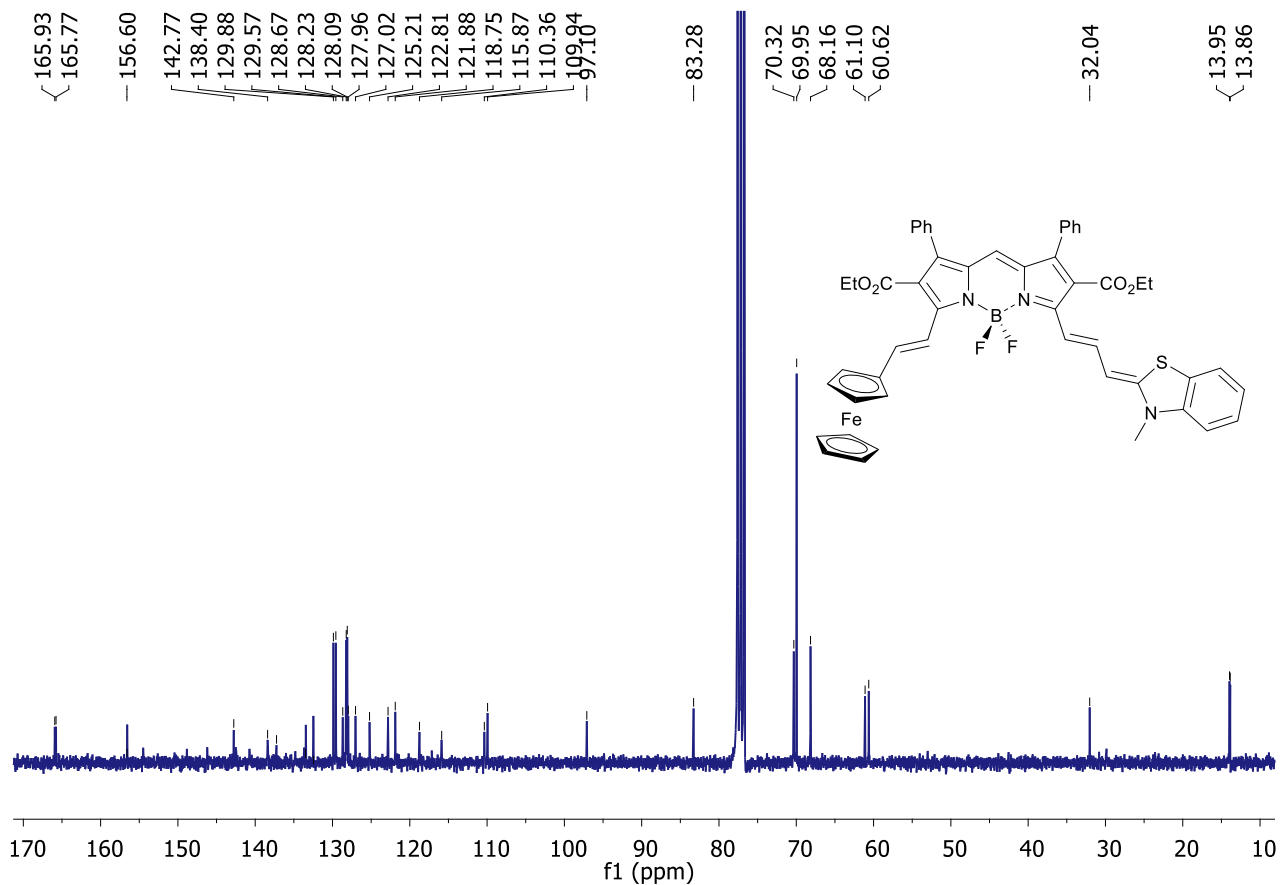


**Figure S15.** <sup>13</sup>C NMR spectrum of compound **6** in CDCl<sub>3</sub>.

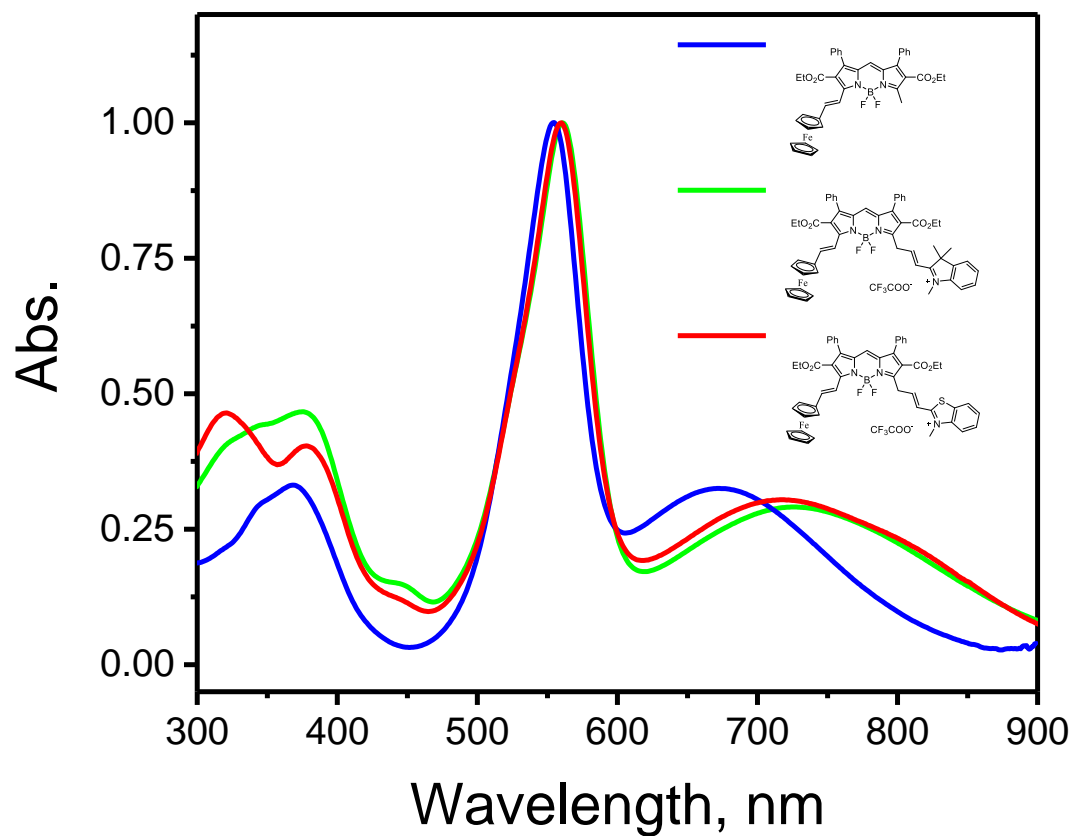


**Figure S16.** The comparison of the normalized UV-vis spectra of protonated dyes  $[5+H]^+$  and  $[6+H]^+$  with Fc-BODIPY dyad.



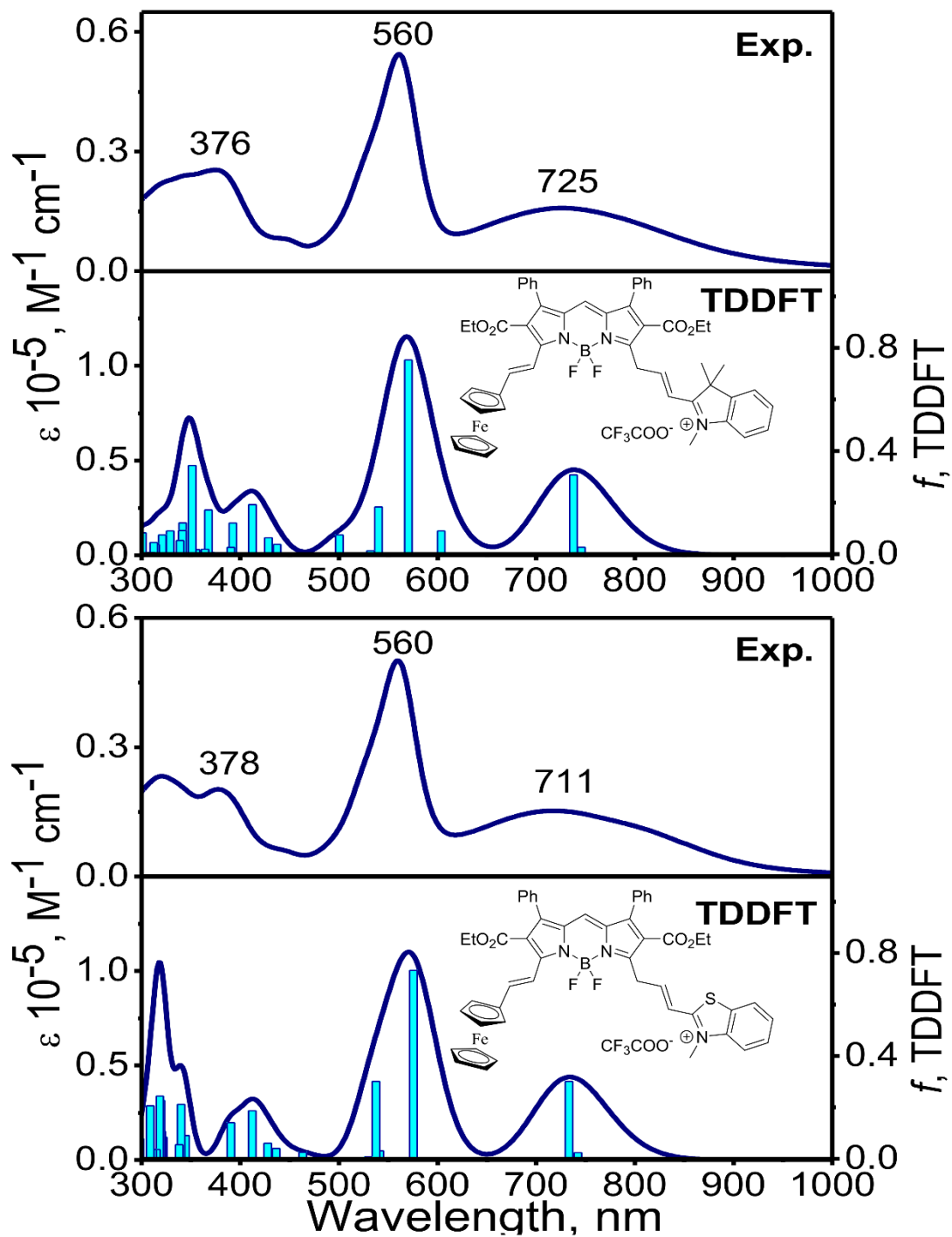


**Figure S17.** UV-Vis-NIR (top), and TDDFT-predicted (bottom) UV-vis spectra of protonated dyes  $[5+H]^+$  and  $[6+H]^+$ .

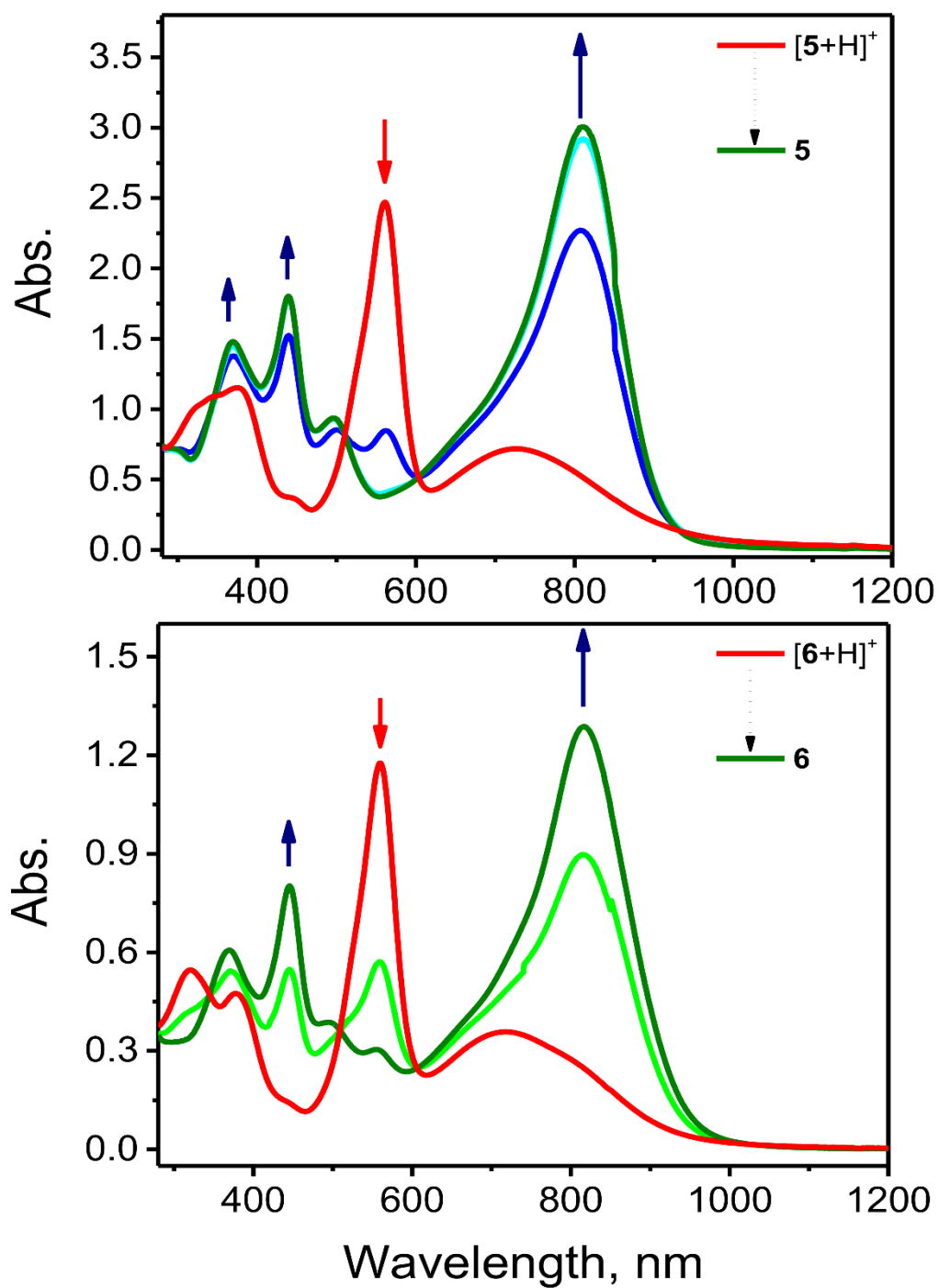


**Figure S18.** Transformation of  $[5+H]^+$  (top) and  $[6+H]^+$  (bottom) into corresponding **5** and **6** under TEA titrations in DCM.

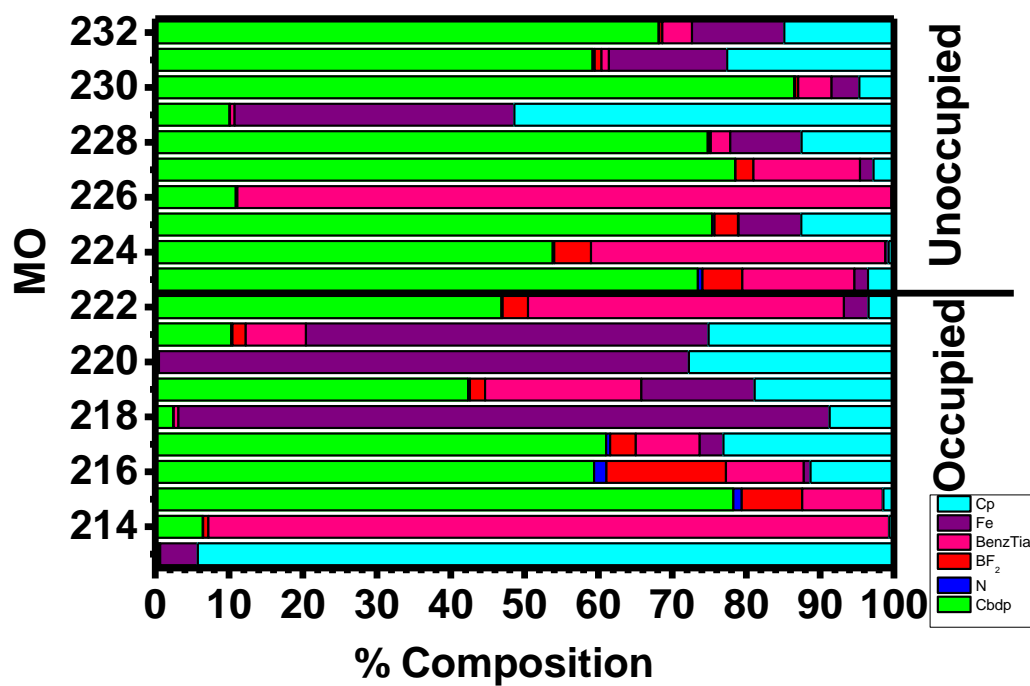
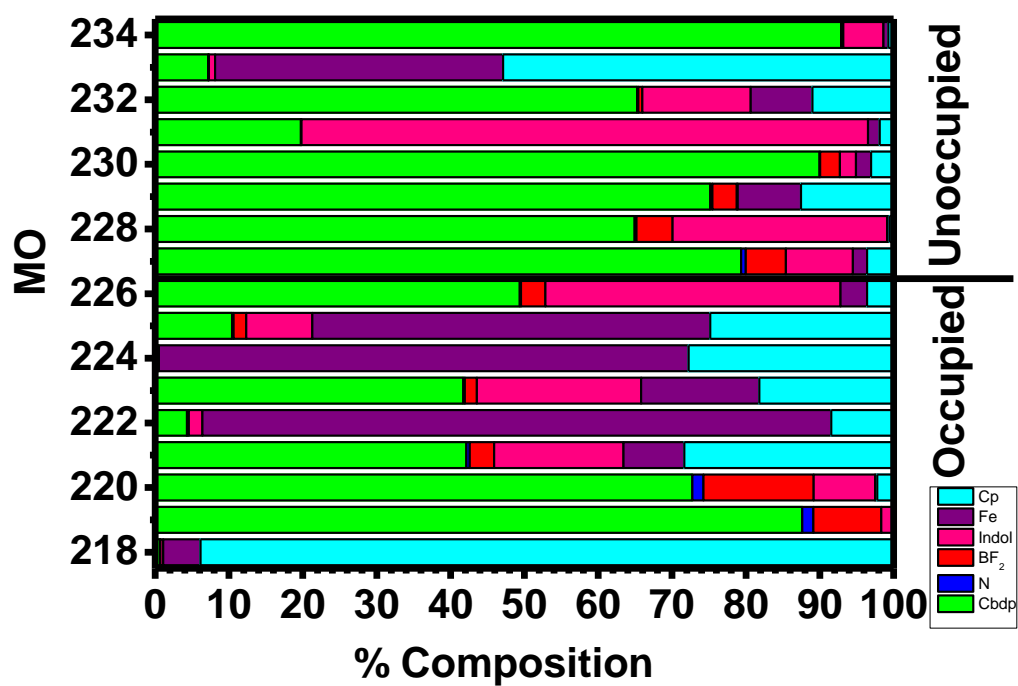
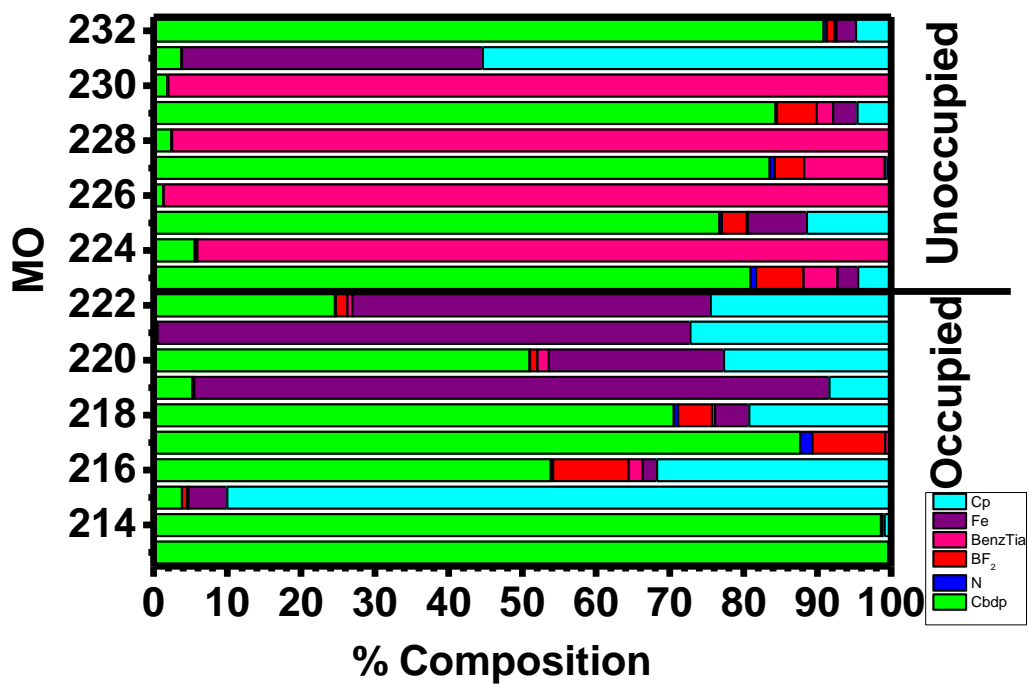
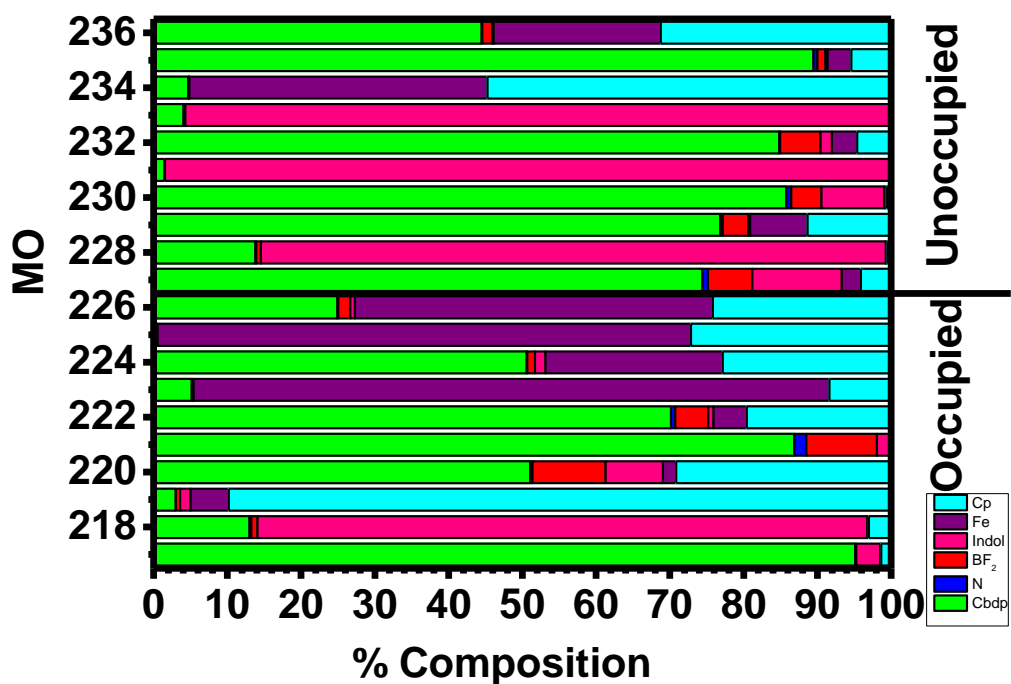


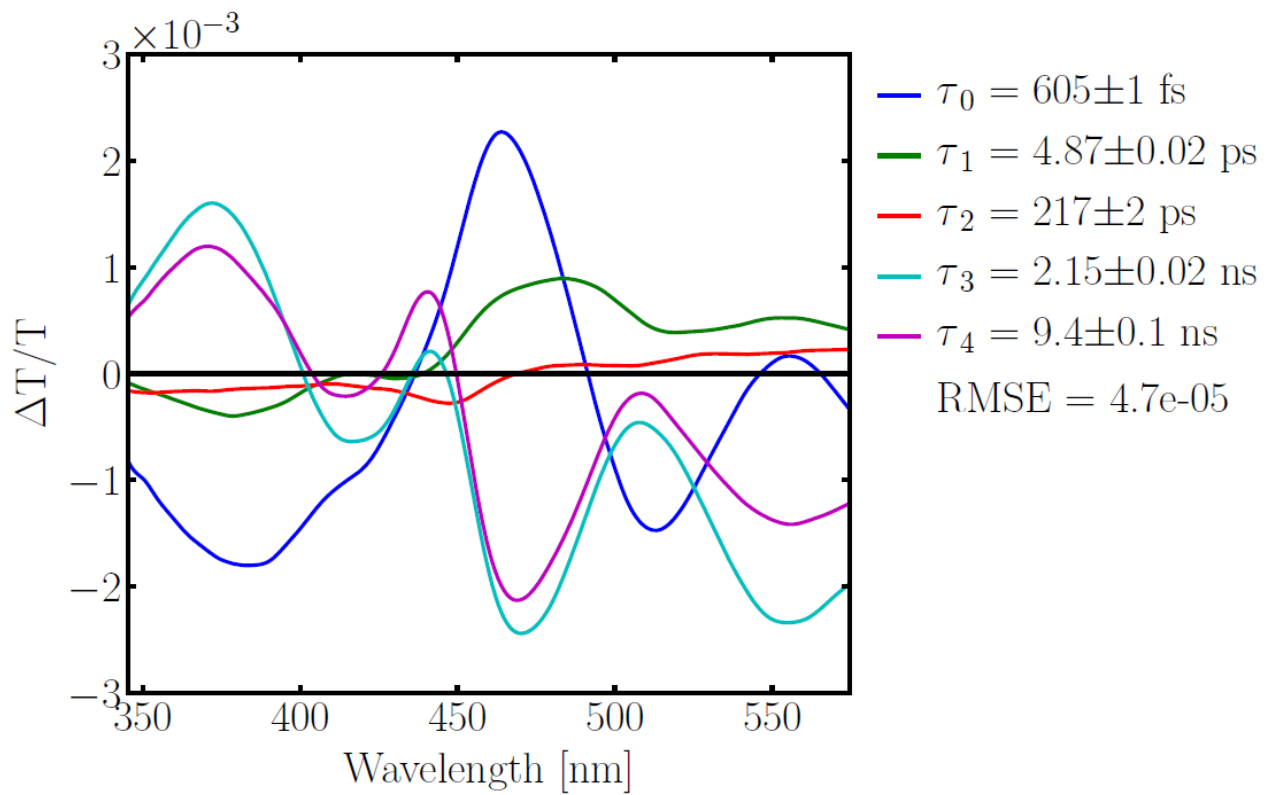
Figure S19. DFT SP predicted MOs composition for triads 5 (top) and 6 (bottom).



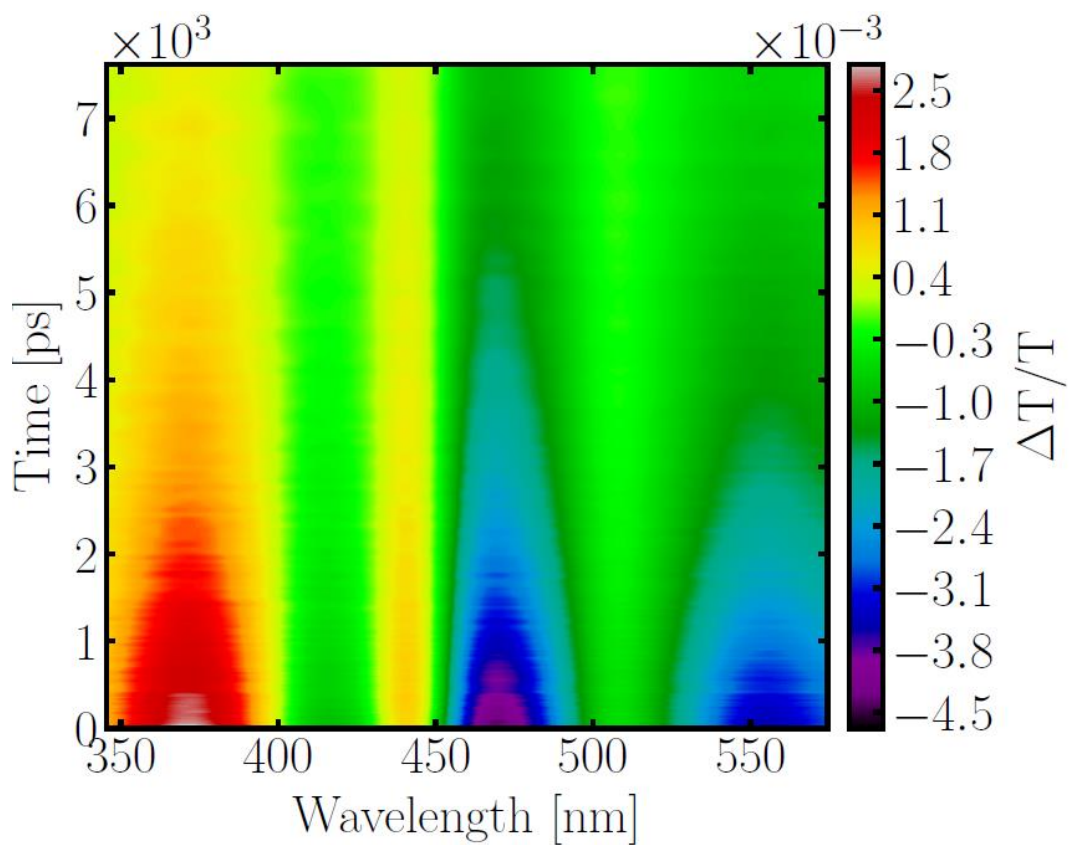
**Figure S20.** DFT SP predicted MOs composition for protonated dyes [5+H]<sup>+</sup> (top) and [6+H]<sup>+</sup> (bottom).

$E_p = 500\text{pJ};$   
 $d_p = \sim 200\mu\text{m};$

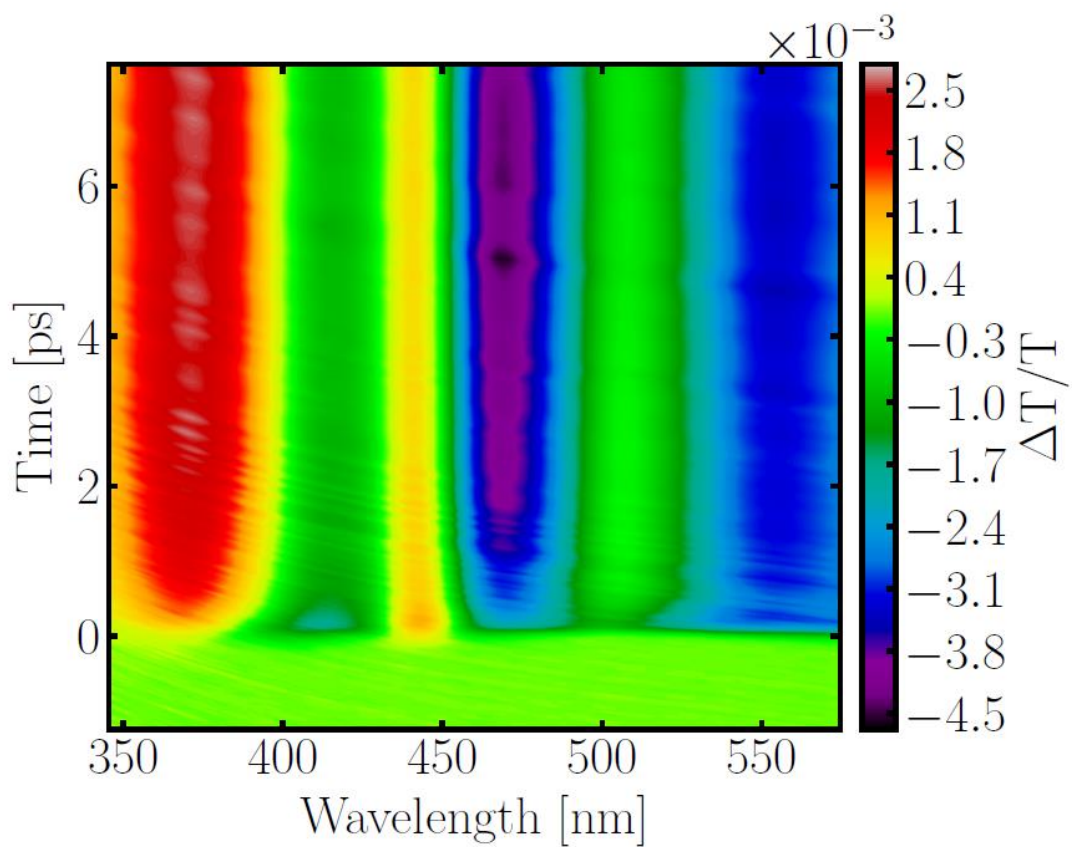
$T = 298\text{K};$   
 $\text{IRF} = 79\text{fs}$



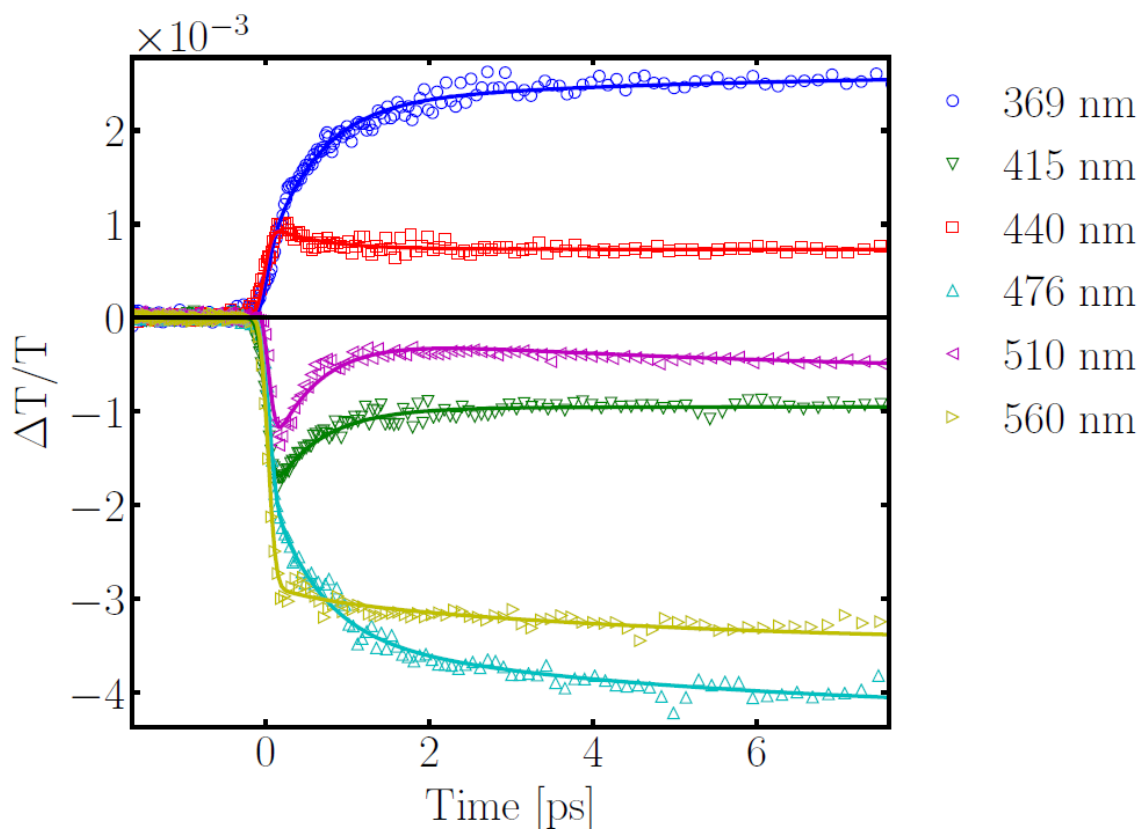
**Figure S21.** Decay associated spectra of **5** ( $\lambda_p=800\text{nm}$ ,  $\lambda_{pr}=460\text{nm}$ ).



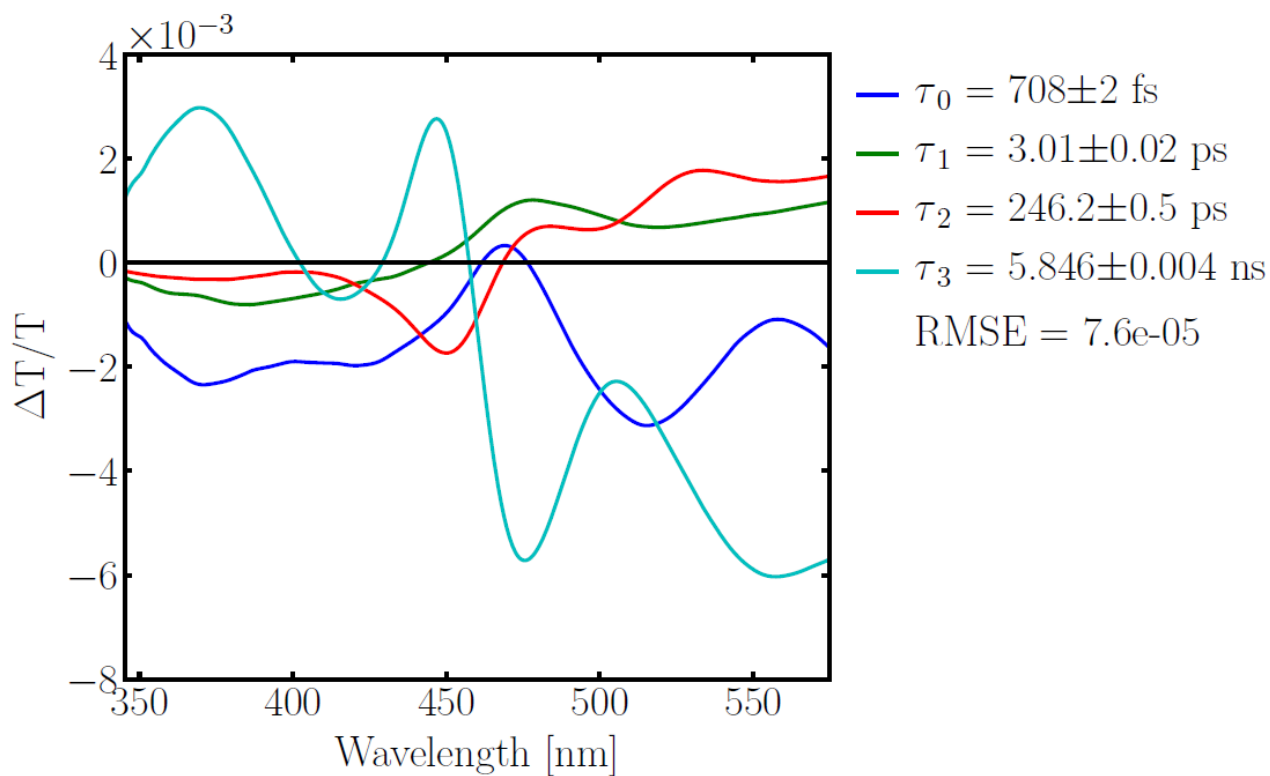
**Figure S22.** Transient absorption map of **5** ( $\lambda_p=800\text{nm}$ ,  $\lambda_{pr}=460\text{nm}$ ) over a 7ns window.



**Figure S23.** Transient absorption map of **5** ( $\lambda_p=800\text{nm}$ ,  $\lambda_{pr}=460\text{nm}$ ) over a 8ps window.

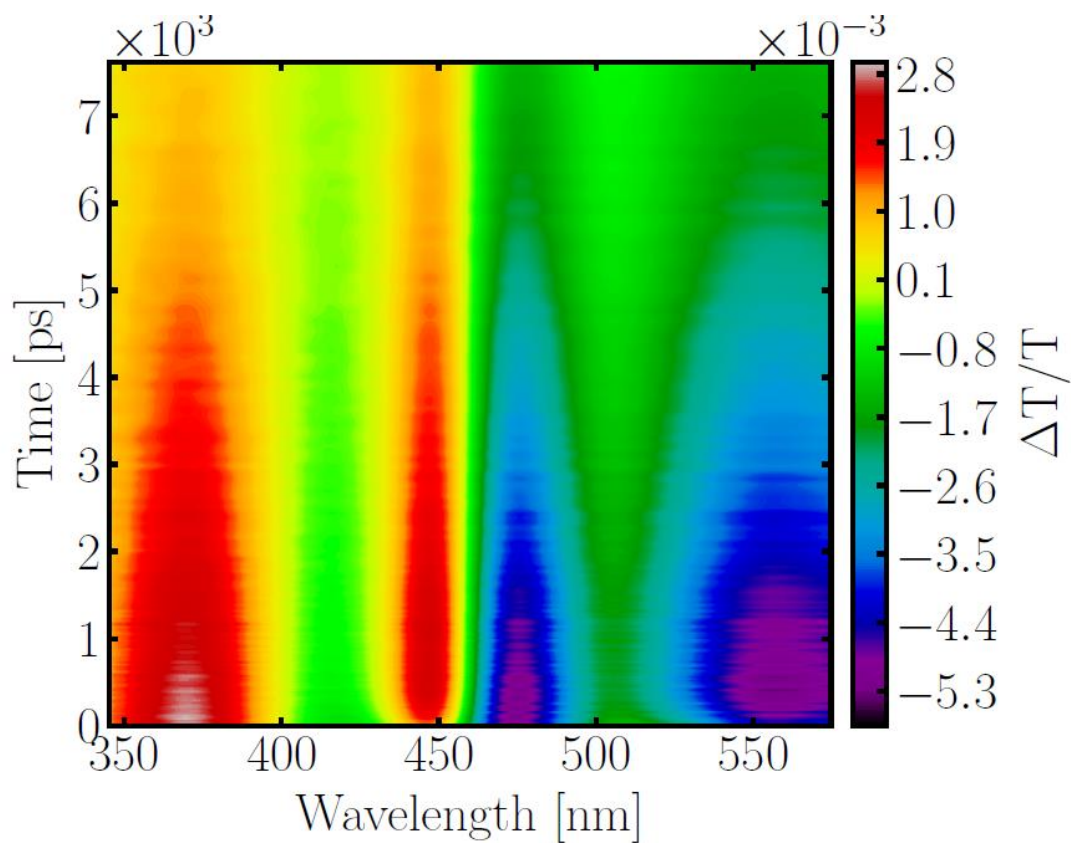


**Figure S24.** Transient absorption kinetics of **5** ( $\lambda_p=800\text{nm}$ ,  $\lambda_{pr}=460\text{nm}$ ) at different wavelengths on an 8ps window.

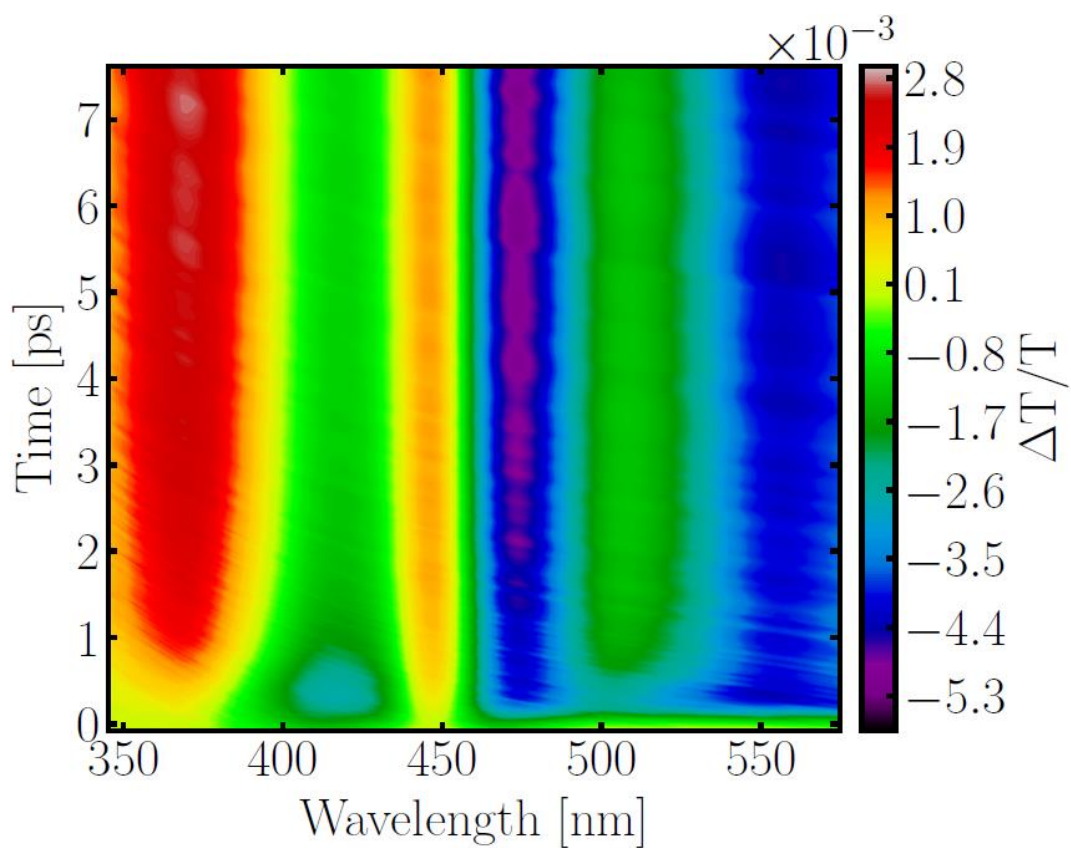


**Figure S25.** Decay associated spectra of **6** ( $\lambda_p=800\text{nm}$ ,  $\lambda_{pr}=460\text{nm}$ ).

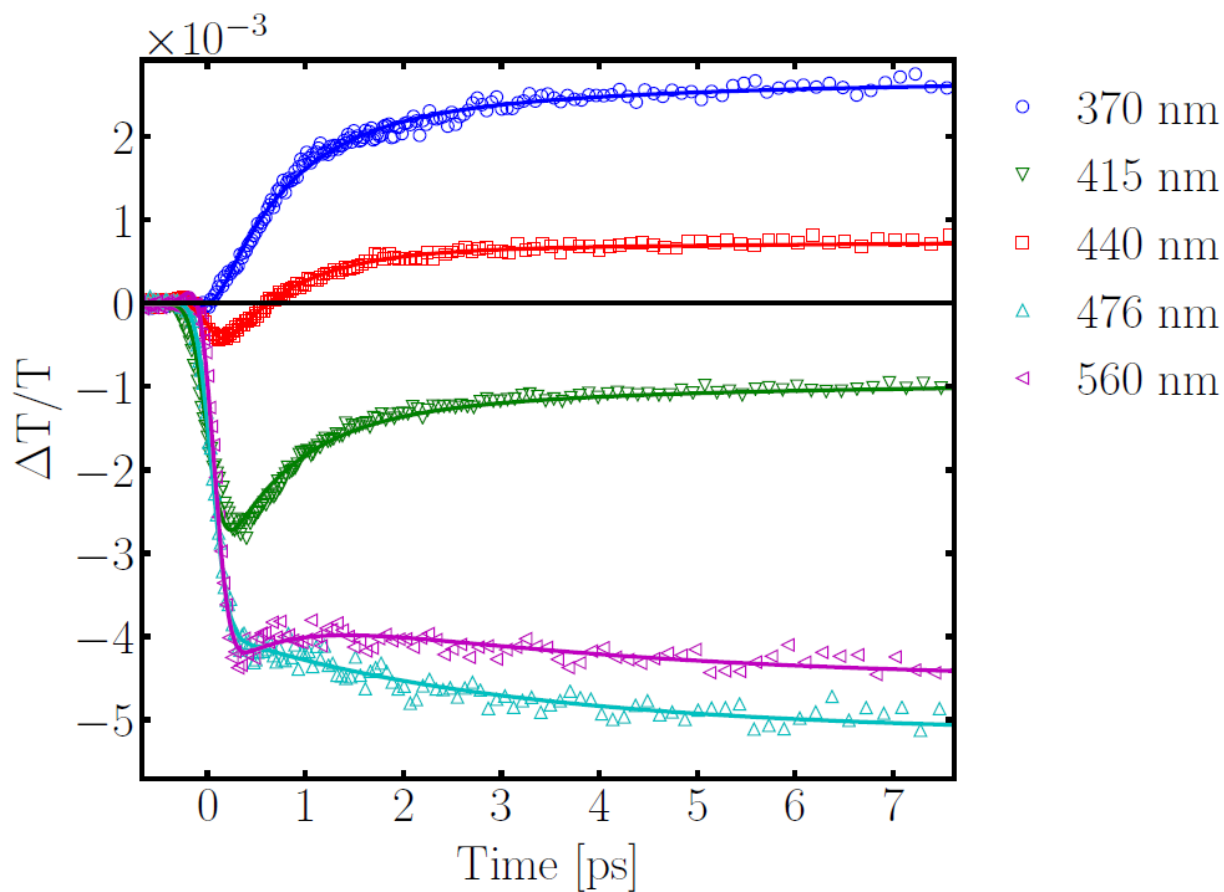




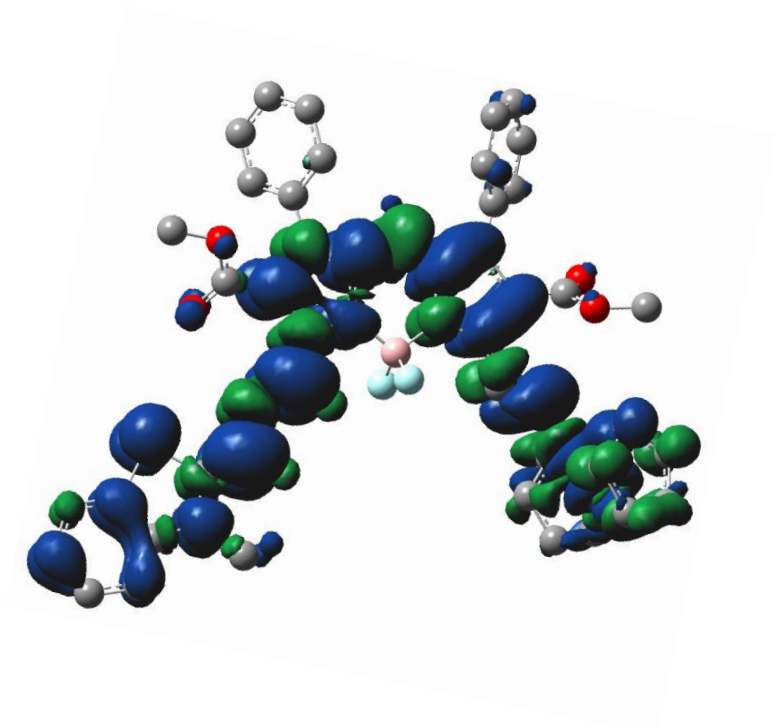
**Figure S26.** Transient absorption map of **6** ( $\lambda_p=800\text{nm}$ ,  $\lambda_{pr}=460\text{nm}$ ) over a 7ns window.



**Figure S27.** Transient absorption spectra of **6** ( $\lambda_p=800\text{nm}$ ,  $\lambda_{pr}=460\text{nm}$ ) at different times.

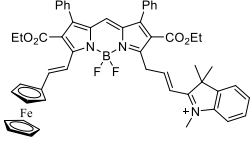
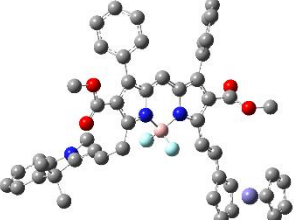
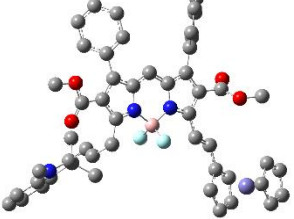
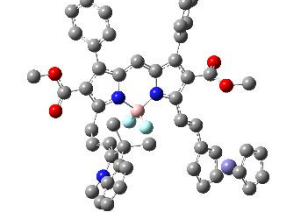
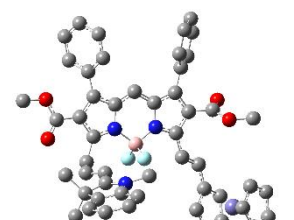
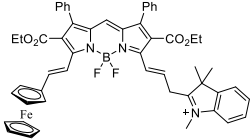
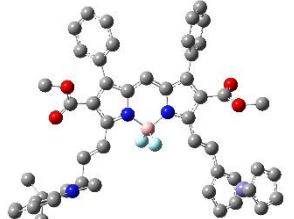
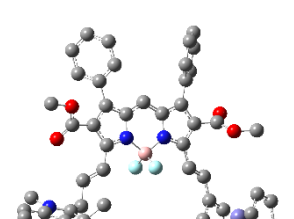


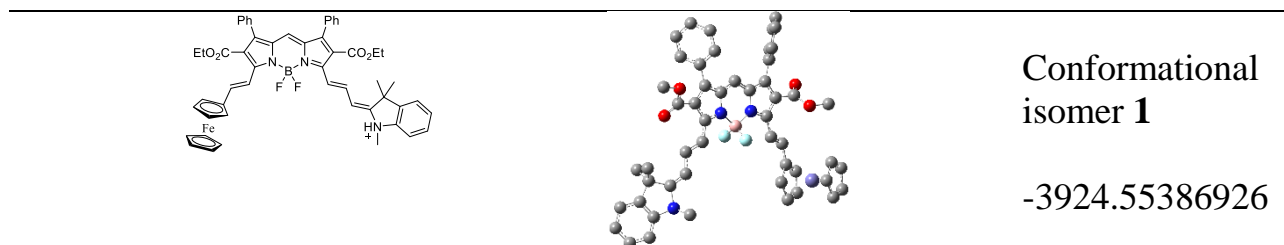
**Figure S28.** Transient absorption kinetics of **6** ( $\lambda_p=800\text{nm}$ ,  $\lambda_{pr}=460\text{nm}$ ) at different wavelengths on an 8ps window.



**Figure S29.** DFT-PCM predicted spin density distribution of cation **6**<sup>+</sup>.

**Table S1.** DFT optimized geometries and their energies off possible protonated isomers of dyes  $[5+H]^+$  and  $[6+H]^+$

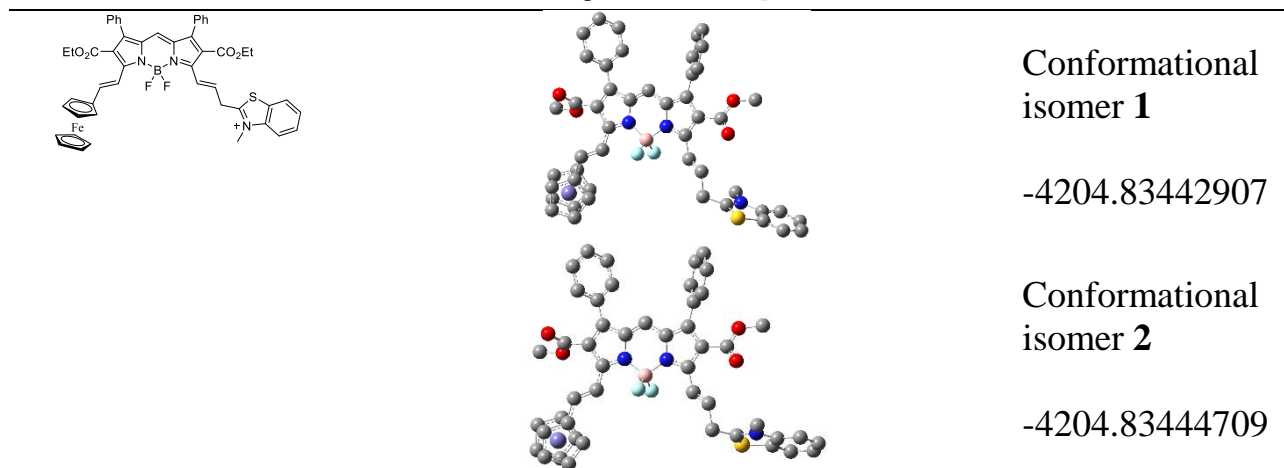
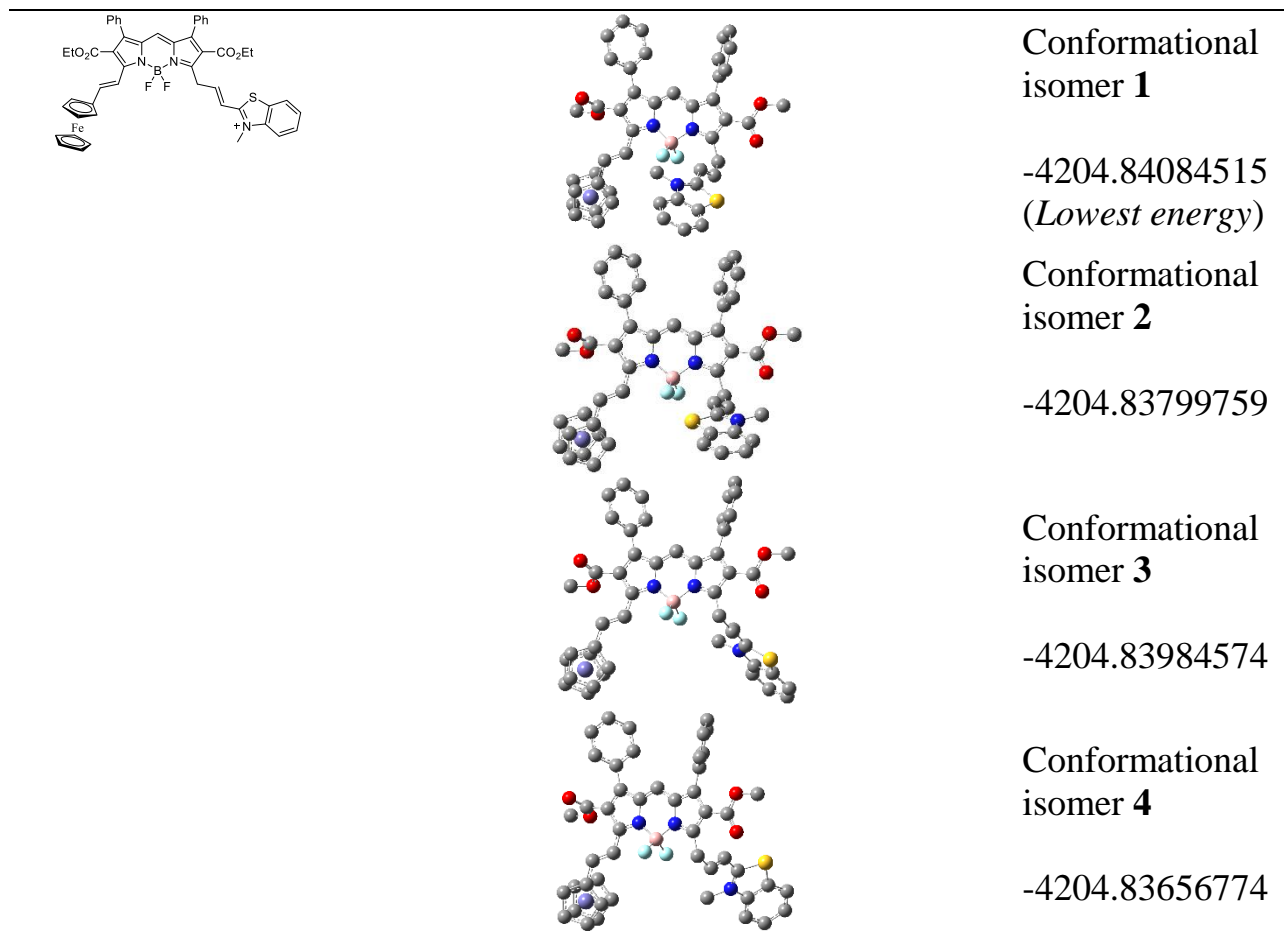
Isomer	Energy, $E_h$
<p style="text-align: center;"><math>[5+H]^+</math></p> <div style="display: flex; justify-content: space-between;"> <div style="width: 25%;">  </div> <div style="width: 50%; text-align: center;">  </div> <div style="width: 25%; text-align: right;"> <p>Conformational isomer <b>1</b></p> <p>-3924.58466167 <i>(Lowest energy)</i></p> </div> </div> <div style="display: flex; justify-content: space-between; margin-top: 20px;"> <div style="width: 25%;"></div> <div style="width: 50%; text-align: center;">  </div> <div style="width: 25%; text-align: right;"> <p>Conformational isomer <b>2</b></p> <p>-3924.58459549</p> </div> </div> <div style="display: flex; justify-content: space-between; margin-top: 20px;"> <div style="width: 25%;"></div> <div style="width: 50%; text-align: center;">  </div> <div style="width: 25%; text-align: right;"> <p>Conformational isomer <b>3</b></p> <p>-3924.58121234</p> </div> </div> <div style="display: flex; justify-content: space-between; margin-top: 20px;"> <div style="width: 25%;"></div> <div style="width: 50%; text-align: center;">  </div> <div style="width: 25%; text-align: right;"> <p>Conformational isomer <b>4</b></p> <p>-3924.58399575</p> </div> </div>	
<div style="display: flex; justify-content: space-between;"> <div style="width: 25%;">  </div> <div style="width: 50%; text-align: center;">  </div> <div style="width: 25%; text-align: right;"> <p>Conformational isomer <b>1</b></p> <p>-3924.57742966</p> </div> </div> <div style="display: flex; justify-content: space-between; margin-top: 20px;"> <div style="width: 25%;"></div> <div style="width: 50%; text-align: center;">  </div> <div style="width: 25%; text-align: right;"> <p>Conformational isomer <b>2</b></p> <p>-3924.57767401</p> </div> </div>	

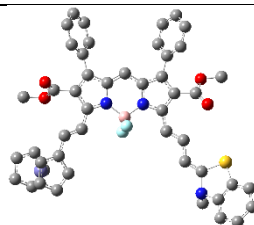
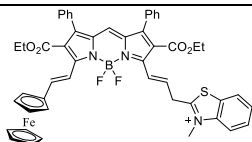


**Isomer**

**Energy,  $E_h$**

**[6+H]<sup>+</sup>**





Conformational  
isomer **1**

-4204.79432430

**Table S2.** Redox properties of triads **5** and **6** in DCM. <sup>[a]</sup>

Dye	Oxidation		Reduction
	$E_{1/2}^{\text{Ox2}}, \text{V}$	$E_{1/2}^{\text{Ox1}}, \text{V}$	$E_{1/2}^{\text{red1}}, \text{V}$
<b>5</b>	0.14	~ 0	-1.20
<b>6</b> <sup>†</sup>	0.12	~ -0.1	-1.24

<sup>[a]</sup> All potentials are referred to the FcH/FcH<sup>+</sup> couple.

## REFERENCES

1. M. P. Shandura, V. P. Yakubovskiy, Y. P. Kovtun, *Org. Biomol. Chem.* 2013, **11**(5), 835-841.
2. O. P. Klochko, I. A. Fedyunyayeva, S. U. Khabuseva, O. M. Semenova, E. A. Terpetschnig, L. D. Patsenker, 2010 *Dyes Pigm.*, **85**(1), 7-15
3. A. D. Becke, *J. Chem. Phys.* 1993, **98**, 5648-5652; b) C. Lee, W. Yang, R. G. Parr, *Phys. Rev. B* 1988, **37**, 785-789.
4. a) C. L. Firme, D. de L. Pontes, O. A. C. Antunes, *Chem. Phys. Lett.* 2010, **499**, 193-198; b) V. Kalamse, N. Wadnerkar, A. Chaudhari, *J. Phys. Chem. C* 2010, **114**, 4704-4709; c) H. A. Meylemans, N. H. Damrauer, *Inorg. Chem.* 2009, **48**, 11161-11175; d) A. Alparone, H. Reis, M. G. Papadopoulos, *J. Phys. Chem. A* 2006, **110**, 5909-5918; e) P. V. Solntsev, S. V. Dudkin, J. R. Sabin, V. N. Nemykin, *Organometallics* 2011, **30**, 3037-3046; f) W. R. Goetsch, P. V. Solntsev, C. Van Stappen, A. A. Purchel, S. V. Dudkin, V. N. Nemykin, *Organometallics* 2014, **33**, 145-157.
5. J. Tomasi, B. Mennucci, R. Cammi, *Chem. Rev.* 2005, **105**, 2999-3093.
6. A. J. H. Wachters, *J. Chem. Phys.* 1970, **52**, 1033-1036.
7. A. D. McLean, G. S. Chandler, *J. Chem. Phys.* 1980, **72**, 5639-5648.
8. *Gaussian 09, Revision D.1*, M. J. Frisch, G. W. Trucks, H. B. Schlegel, G. E. Scuseria, *et al* Gaussian, Inc., Wallingford CT, **2009**.
9. A. L. Tenderholt, *QMForge*, Version 2.1. Stanford University, Stanford, CA, USA.